3-2002

Determination of the Possible Locations of the Receiver on a Passive Coherent Location System, Considering the Effects of the Terrain and the Atmospheric Conditions

Carlos A. Meier

DETERMINATION OF THE POSSIBLE LOCATIONS OF THE RECEIVER ON A PASSIVE COHERENT LOCATION SYSTEM, CONSIDERING THE EFFECTS OF THE TERRAIN AND THE ATMOSPHERIC CONDITIONS

THESIS

Carlos A. Meier, Lieutenant, Chile Air Force

AFIT/GE/ENG/02M-17

DEPARTMENT OF THE AIR FORCE
AIR UNIVERSITY

AIR FORCE INSTITUTE OF TECHNOLOGY

Wright-Patterson Air Force Base, Ohio

Report Documentation Page

Report Date	**Report Type**	**Dates Covered (from... to)**
26 Mar 02	Final	Sept 2001 - Feb 2002

Title and Subtitle Determination of the Possible Locations of the Receiver on a Passive Coherent Location System, Considering the Effects of the Terrain and the Atmospheric Conditions.	**Contract Number**
	Grant Number
	Program Element Number
Author(s) Lt Carlos A. Meier, Chile Air Force	**Project Number**
	Task Number
	Work Unit Number
Performing Organization Name(s) and Address(es) Air Force Institute of Technology Graduate School of Engineering and Management (AFIT/EN) 2950 P Street, Bldg 640 WPAFB OH 45433-7765	**Performing Organization Report Number** AFIT/GE/EG/02M-17
Sponsoring/Monitoring Agency Name(s) and Address(es) Paul E. Howland NATO C3 Agency Surveillance Branch Air C2 Sensors Division P. O. Box 174, 2501 CD The Hague, Netherlands	**Sponsor/Monitor's Acronym(s)**
	Sponsor/Monitor's Report Number(s)

Distribution/Availability Statement
Approved for public release, distribution unlimited

Supplementary Notes
The original document contains color images.

Abstract
It has always been an issue for an armed force, or government, to obtain complete radar coverage over an area of interest. Generally, this objective remains unaccompished due to geographical, technical, and/or operational reasons (meaning topographic obstacles, transmitted power, extremem isolation, hierarchy of objectives, etc.) The fact of having vast areas of territory beyond radar coverage can be decisive in an armed conflict. With the recent resurgence of bistatic radar theory and applications, now in the form of Passive Coherent Location (PCL) systems, using existing signal sources (TC and Radio Stations) it is possible to decrease the blind zones of a country's air defense system, in a somehow economic and effective way. The general purpose of this thesis is to develop a methodology to determine possible receiver locations needed to implement a PCL system, while emphasizing low altitude coverage, specific terrain and atmospheric information, available signal sources and the needed for coverage.

Subject Terms
Radar, Passive Sensors, Radar Site Analysis, Atmospheric Propagation Loss

Report Classification unclassified	**Classification of this page** unclassified
Classification of Abstract unclassified	**Limitation of Abstract** UU
Number of Pages 117	

The views expressed in this document are those of the author and do not reflect the official policy or position of the United States Air Force, Department of Defense, United States Government, the corresponding agencies of any other government, NATO, or any other defense organization.

This document represents the results of research based on information obtained solely from open sources. No agency, whether United States Government or otherwise, provided any threat system parameters, or weapons systems performance data in support of the research documented herein.

AFIT/GE/ENG/02M-17

DETERMINATION OF THE POSSIBLE LOCATIONS OF THE RECEIVER ON A PASSIVE COHERENT LOCATION SYSTEM, CONSIDERING THE EFFECTS OF THE TERRAIN AND THE ATMOSPHERIC CONDITIONS

THESIS

Presented to the Faculty of the Department of Electrical and Computer Engineering

Graduate School of Engineering and Management

Air Force Institute of Technology

Air University

Air Education and Training Command

In Partial Fulfillment of the Requirements for the

Degree of Master of Science in Electrical Engineering

Carlos A. Meier, B.S.

Lieutenant, Chile Air Force

March 2002

Acknowledgements

Beneath this page lays the work, effort and encouragement of many people who helped and supported me during this endeavor. First, I would like to thank my thesis advisor, Dr. Andrew Terzuoli, who gave life to this project. His constant enthusiasm and support gave me the base to build upon. I would also like to thank Dr. Michael Temple for his patience, time, and clear answers to my endless questions.

I wish to acknowledge the great support received from Mr. Ray Wasky. He generously dedicated his time and shared his knowledge with me, which contributed immensely to the success of this research.

I also want to thank my classmates Kerim Say, Baris Calikoglu, Abdulkhadir Guner, and Ahmet Ozcetin for their friendship and encouragement.

Finally, I wish to thank my beloved and loving wife, who was my teammate in this effort. Her infinite support and solid faith in me, helped me to see this project through to completion.

Carlos A. Meier

Table of Contents

Page

Acknowledgments……..iv
List of Figures…...…….vii
List of Tables……..ix
Abstract……x

I. Introduction……1-1

1.1 Background....1-1
1.2 Problem Statement....1-2
1.3 Summary of Current Knowledge....1-2
1.4 Assumptions....1-4
1.5 Scope....1-5
1.6 Approach....1-6
1.6.1 Literature Review....1-6
1.6.2 General Scenario....1-6
1.6.3 The Transmitter-To-Receiver.....1-6
1.6.4 The Transmitter-To-Object....1-6
1.6.5 The Object -To-Receiver.....1-7
1.6.6 Difining the Location of the Receiver.....1-7
1.7 Thesis Organization....1-7

II. Literature Review…… 2-1

2.1 Introduction....2-1
2.2 The Bistatic Radar....2-2
2.2.1 History.....2-2
2.2.2 The Bistatic Radar Equation.....2-4
2.2.3 The Bistatic Geometry.....2-9
2.3 Advanced Refractive Effects Prediction System (AREPS)....2-12
2.3.1 Flat Earth Ray Optic Region....2-13
2.3.2 The Ray Optic Region.....2-14
2.3.3 The Parabolic Equation Region.....2-14
2.3.4 The Extended Optic Region....2-18
2.4 Refraction....2-19
2.5 Meteorological Data....2-22
2.6 Digital Terrain Characterization....2-23
2.7 Transmitter Parameters....2-26
2.8 Receiver Parameters....2-27
2.9 Object Parameters....2-31
2.10 Summary....2-31

Page

III. Methodology……..3-1

3.1 Introduction.....3-1
3.2 General scenario 3-1
3.2.1 The Terrain 3-1
3.2.2 The Meteorological Conditions 3-9
3.2.3 The Transmitter. 3-10
3.2.4 The Object 3-11
3.3 The Transmitter-To-Receiver Path 3-12
3.3.1 The Direct Signal Without the Effects of the Receiver Antenna Pattern 3-12
3.3.2 Adding the Effects of the Receiver Antenna Pattern.....3-22
3.4 The Transmitter-To-Object Path.....3-26
3.5 The Object-To-Receiver Path 3-28
3.6 The Location of the Receiver 3-36
3.7 Summary.....3-38

IV. Results and Analysis…….. 4-1

4.1 Introduction.....4-1
4.2 General scenario 4-1
4.3 Meteorological Summary 4-2
4.4 The Direct Signal without the Effects of the Receiver Antenna Pattern. 4-3
4.5 Adding the Receiver Antenna Pattern Effects. 4-6
4.6 The Transmitter-To-Object Path.....4-9
4.7 The Object-To-Receiver Path 4-10
4.8 The Receiver Location.....4-13
4.9 Summary.....4-15

V. Conclusions and Future Work……5-1

5.1 Conclusions.....5-1
5.2 Future Work.....5-6

Appendix A: Matlab® Codes……..APPEND-1

Bibliography…… BIB-1

Vita……VITA-1

-

List of Figures

Figure Page

2.1 Monostatic and Bistatic configurations....2-4
2.2 North-referenced coordinate system. 2-9
2.3 Ovals of Cassini. 2-10
2.4 APM calculations regions. 2-13
2.5 Refractive conditions. 2-22
2.6 Digital terrain characterization....2-24
2.7 Receiver antenna pattern. 2-29
2.8 Effects of the direct signal on the receiver before and after filtering....2-30
3.1 Grid and coordinate system, including the quadrant identifiers. 3-2
3.2 Terrain profile at 90º including the main elevation values and its coordinates 3-4
3.3 Matrices layout. 3-5
3.4 Terrain profile generated using interpolation....3-8
3.5 Terrain profile using the nearest values to the desired bearing....3-8
3.6 Elevation vectors plotted on top of the terrain surface 3-8
3.7 AREPS *research* window 3-8
3.8 AREPS Decision Aid window 3-8
3.9 AREPS Range vs. Propagation Loss window....3-15
3.10 The loss vectors layout....3-18
3.11 Matching the size of the **LH** matrices....3-19
3.12 The **RHO** and **θ** matrices. 3-20
3.13 Obtaining a single **LD** matrix....3-21
3.14 Obtaining the **LD** matrix for the whole terrain 3-22
3.15 Geometry to calculate the angle of the antenna pattern with respect to the maximum direction of gain, *az*....3-24
3.16 The geometry for the Transmitter-to-Object path. 3-27
3.17 The new coordinate system, centered at the AOI 3-29
3.18 The angle θ_R, assigned to the terrain files....3-30
3.19 Calculating the Object-to-Receiver path at a particular bearing....3-33
4.1 Representation of the first quadrant of the terrain surface....4-2
4.2 Summary of the propagating conditions 4-3
4.3 Signal propagation losses, in dB, from the transmitter, within the first quadrant 4-4
4.4 Signal propagation loss at 20m above the ground level....4-6
4.5 Receiver antenna gain at the angle of arrival of the direct signal 4-6
4.6 Received power of the direct signal, including the effects of the receiver antenna...4-9
4.7 Signal propagation losses from the object, within the first and fourth quadrant 4-11
4.8 Signal propagation loss at 20m above the ground level....4-12
4.9 Received power of the indirect signal....4-13

Figure Page

4.10 Indirect signal power above the receiver threshold. 4-14
4.11 Indirect signal power level above the direct signal power level 4-14
4.12 Terrain coordinates to locate the receiver of a PCL system....4-15
5.1 Bistatic angle as a function of the receiver location 5-3
5.2 Quasi-monostatic region 5-4
5.3 The angle formed by the object velocity vector and the bistatic bisector, and the resulting Doppler shift. 5-5

List of Tables

Table Page

3.1 Transmitter parameters 3-11

Abstract

It has always been an issue to obtain complete radar coverage over an area of interest. Generally, this objective remains unaccomplished due to geographical, technical, and/or operational reasons (meaning topographic obstacles, transmitted power, extreme isolation, hierarchy of objectives, etc.). The fact of having vast areas of territory beyond radar coverage can be devastating.

With the recent resurgence of bistatic radar theory and applications, now in the form of Passive Coherent Location (PCL) systems, using existing signal sources (TV and Radio stations) it is possible to decrease the blind zones in a somehow economic and effective way.

The general purpose of this thesis is to develop a methodology to determine possible receiver locations needed to implement a PCL system, while emphasizing low altitude coverage, specific terrain and atmospheric information, available signal sources and the need for coverage.

DETERMINATION OF THE POSSIBLE LOCATIONS OF THE RECEIVER ON A PASSIVE COHERENT LOCATION SYSTEM, CONSIDERING THE EFFECTS OF THE TERRAIN AND THE ATMOSPHERIC CONDITIONS

I. Introduction

1.1 Background

Having vast areas of territory out of radar coverage can be devastating. It has always been an issue to give complete radar coverage within an area of interest. Generally, this objective remains unfulfilled due to geographical, technical, and/or operational reasons (i.e., topographic obstacles, transmitted power, extreme isolation, hierarchy of objectives, etc.).

In a typical case, the surveillance system is implemented using monostatic radars covering a general area, and normally, because of geographic obstructions like mountains or other terrain features, there would be blind zones where object detection is impossible due to the limited radio electric horizon. A possible solution to this problem is to populate the blind areas with gap fillers or short-range radars designed for this purpose.

Another solution to the problem is using a Passive Coherent Location (PCL) system to fill these gaps, which is the object of this thesis.

A PCL system is a type of bistatic or multistatic radar configuration, which in simple terms, is a radar that uses as a transmitter one or more existing sources, such as television or radio stations, and one or more receivers located at a considerable distance with respect to the distance from an object intended to be detected. This technology constitutes the latest

resurgence of bistatic and multistatic radar theory and their applications, making it possible to decrease blind zones of radar systems, in an economic and effective way.

1.2 Problem Statement

One of the problems to solve in an air surveillance scenario is to detect, as early as possible, low flying object using the geographic environment as a shield against radar emission.

This research looks at the geometry of television based bistatic radar. Specifically, at the possible location(s) for the receiver(s) with respect to the transmitter and one general Area of Interest (AOI) to accomplish early detection of low-level flying object. The problem will be solved within a given scenario, using a digital terrain simulation, the local atmospheric characteristics, and a set of initial assumptions.

The solution space (the set of points where the receiver could perform its task) is driven by assuming the necessity of providing early low-level coverage detection as the main requirement. In other words, the receiver will be placed where low-level coverage is enhanced. A final objective of this thesis is to analyze, based on certain operational considerations, the level of usefulness of the possible receiver sites for some specific cases.

1.3 Summary of Current Knowledge

Several authors who each emphasized different aspects have addressed the design and configuration of various PCL systems. One of the most complete documents written in this area is the PhD thesis “Television Based Bistatic Radar” written by Howland [1]. He

focuses on the process of detecting and tracking objects using, in one of his practical experiences, the vision carrier of a domestic television broadcast with a vestigial side band modulation scheme. He measures the Doppler shift and the direction of arrival (DOA) of the signal, develops the necessary algorithms to identify the object echoes and then initiates the tracking of them. Howland describes the characteristics and the geometry of the system implemented to support his research. The assumptions include a flat earth; therefore, the issues related to propagation losses due to the terrain and atmospheric propagation are not addressed; they are beyond the scope of his thesis.

In the conclusions of the aforementioned document, Howland states: "the use of terrestrial television broadcast to act as an illuminator for a bistatic radar system has been successfully demonstrated" [1:222]. The above, along with the claimed success of similar experiments by private companies, motivates this research and constitutes the basic assumption that a PCL system can accomplish detection of airborne objects.

Another main source considered in the area of this thesis is the book "Bistatic Radar" by Willis [2]. Even though he does not specifically address the PCL application, the author gives a complete and detailed description of the geometry and the considerations of bistatic radar systems in general.

Finally, since the problem of this research involves geographic terrain features and atmospheric conditions, the use of a propagation model that includes these parameters is needed. The software used is the "Advanced Refractive Effects Prediction System" (AREPS) [4, 5], based on the "Advanced Propagation Model"(APM) [3]. This software was designed at the Space and Naval Warfare Systems Center, Atmospheric Propagation Branch, and based in the Parabolic Equation model [6, 7, 8, 9]. AREPS provides signal

losses versus range at selected azimuth angles over a customized terrain or over real terrain digital data, considering the effects of terrain and the atmospheric conditions in the region. It also allows for generating files with horizontal propagation loss profiles at different altitudes and/or vertical propagation loss profiles at different ranges.

1.4 Assumptions

The following is a list of the necessary assumptions to establish the starting point of this research.

- The PCL system is intended to provide short-to-medium range air surveillance.
- The receiver location will tend to benefit the low-level coverage.
- The analysis considers a single transmitter, located in own territory and continuously transmitting.
- There is not any other transmitter in the vicinity or a considerable noise source nearby.
- The analysis first considers a single receiver. If the intended coverage is accomplished, a second receiver is not needed. This is to minimize cost and complexity in the Digital Signal Processing (DSP) software.
- The receiver antenna and its figures of merit are modeled using an arbitrary pattern.
- The energy to feed the electric systems at the receiver location as well as any other logistic and operational considerations are assumed solved.

– The object has a non-fluctuating radar-cross-section (RCS) of 10 m^2. Specific objects are not considered in this research.

– The coordinate system is the Cartesian plane or North referenced coordinate system where applicable.

– The unit system is the International System.

1.5 Scope

This research addresses the problem of locating the receiver components of a bistatic PCL system, which can be extended to multistatic in case a single receiver is not enough to provide the needed coverage. The solution considers the propagation losses due to atmospheric propagation and losses caused by the terrain. The goal is to determine, as accurately as possible, the receiver position for a PCL system, considering the signal-to-noise ratio (SNR) at the receiver antenna, necessary to provide the input needed for a process like the one described in [1], to take place.

The object tracking problem and techniques are not addressed here. The purpose of this thesis is to accomplish a realistic level of signal-to-noise ratio at the possible receiver location to allow measuring the Doppler shift and DOA. This level of signal-to-noise ratio is considered since the above are inputs to the method used in [1] to accomplish detection and tracking, and it has been proven to work. The data input at the receiver will be of the same format. In other words, the scope of the thesis considers the definitions of the hardware parameters, not the digital signal processing aspects.

1.6 Approach

To solve the problem stated above, the following steps are considered:

1.6.1 Literature Review. Review the literature on the following topics: Technical considerations on the physical location of the receiver on bistatic systems and bistatic geometry in general, the *Parabolic Equation* as a model to calculate propagation losses, and existing papers on PCL system implementation.

1.6.2 General Scenario. Define the general scenario, including the geographic and atmospheric parameters, signal availability and the receiver features, characteristics of the object, and the location of the AOI.

1.6.3 The Transmitter-To-Receiver Path. Calculate the strength of the direct signal from the transmitter. This calculation will be made at every point in the terrain. This will establish the sectors where the direct signal from the transmitter has the adequate level of power to allow a coherent operation of the receiver, and at the same time not cover the signal coming from the object.

1.6.4 The Transmitter-To-Object Path. Calculate the signal strength from the transmitter at the AOI.

1.6.5 The Object-To-Receiver Path. Calculate the signal strength from the object at every point in the terrain and establish the regions where the receiver could possibly be located.

1.6.6 Defining the Receiver Location. Define the possible locations of the receiver according to technical and operational requirements.

1.7 Thesis Organization

This thesis consists of five main chapters and one appendix. Chapter II presents a brief review of the history of bistatic radar, the pertinent theory of bistatic radar, propagation model of electromagnetic waves, meteorological factors that affect the propagation, and the constitutive elements of the systems: the transmitter, the receiver, and the object. Chapter III describes in depth the methodology and proposes the model used to obtain the results and reach a conclusion. Chapter IV details the simulation and analysis of the resulting output obtained by following the methodology detailed in Chapter III. Finally, Chapter V states the conclusions, and proposes future research topics originating from this thesis.

II. Literature Review

2.1 Introduction

This chapter describes the theoretical basis of the research into PCL systems and the way they are implemented given specific terrain information, available signal sources, and the need for coverage.

A PCL system, as described previously, is a type of bistatic radar configuration. In simple terms it is a radar that uses as a transmitter an existing source, such as a television or radio station, and a receiver located at a significant distance from and object of interest.

To implement a system as the one described above, given the location of the transmitter and the area where the object detection is intended, one needs to define the geographic coordinates of the receiver. This is done by considering the fact that the electromagnetic wave once *launched* by the transmitter will suffer changes in its energy and direction of propagation due to the characteristics of the terrain and the atmosphere. Then it will scatter from the object, and will need to arrive with enough energy to allow the receiver to make the necessary measurements to calculate the object parameters.

First, I present the basic theory and the geometry that supports and gives an understandable perspective to bistatic radar. This section will set the theoretical characteristics of the location and characteristics of the receiver.

Second, the most relevant aspects of the components of the system are described, such as the transmitter, the receiver, and the object of interest.

Third, an overview of the theory behind the software used to predict the propagation loss of the electromagnetic waves is portrayed. Finally, the characteristics of the data

needed to make the aforementioned computational tool run, namely, the terrain elevation and the meteorological records are also described.

2.2 The Bistatic Radar

2.2.1 History. The history of radar starts with accidental discoveries leading to the fact that detection of objects was possible when a transmitter would emit electromagnetic waves in the direction of those objects and the waves were reflected by them and captured by a receiver. As stated by Willis [2], most of those *accidents* (later, experiments) were of the bistatic type. The invention of the duplexer in 1936 allowed the researchers to focus on the pulsed monostatic radar.

Since the late 1980's the concept of bistatic and multistatic radar using TV or radio broadcast stations has been addressed numerous times. Howland [1] demonstrated experimentally the feasibility of the implementation of a *Television Based Bistatic Radar* by using broadcasted TV signals and *off-the-shelf* equipment to build the receiver and processing system. The data obtained by the system in several trials was compared with the data provided by a secondary surveillance radar. The results proved the usefulness of the system.

Advantages of the PCL concept with respect to monostatic systems and bistatic systems that use monostatic radar as a source are many. Among these worth mentioning are the following:

- The system operates in frequency bands out of the range of conventional Radar Warning Receivers (RWR). Therefore, the operation of a PCL system is covert.

– The geometry allows exploiting increased radar observability characteristics of an object, especially when located between the receiver and transmitter.

– The fact that the transmitter is *already there* and only a receiver needs to be added to the system lowers the cost and simplifies the implementation.

– The receiver cannot be located by directional finding methods.

– Due to the above, jamming techniques are more complex and often less effective.

There are some PCL disadvantages as well, including:

– The transmitter waveform is designed for its primary use (TV or radio broadcast) and does not necessarily contain the desired features of a radar signal.

– The *hitchhiker* can control neither the power level nor other transmitter parameters.

– The location and tracking accuracy are poor. Implemented systems have located 30% of the estimates of tracks on top of the real track of a object.[1:206]

– Reduced spatial coverage.[2:12]

– Degraded resolution and accuracy in range, Doppler, and angle.[2:12]

In general, it is important to note that there are several different types of monostatic radars, such as surveillance, tracking, Synthetic Aperture Radar (SAR), Inverse SAR (ISAR), etc. The PCL concept is just another kind of Radio Detection and Ranging (RADAR). PCL systems, as well as other bistatic or multistatic systems, are not destined to replace or compete with monostatic radars but rather to supplement them. They can represent a solution for specific problems under particular circumstances.

2.2.2 The Bistatic Radar Equation. As a starting point, as will be demonstrated, the bistatic radar equation and all the calculations derived from it should comply with the fact that when the distance from the transmitter to the receiver is set to 0 the values obtained should correspond to those of a monostatic radar. This comment is made on the basis that most people are more familiar with the monostatic geometry than the one to be used throughout this thesis. Figure 2.1 exemplifies the difference between the two configurations and shows some of the parameters to be used throughout this research.

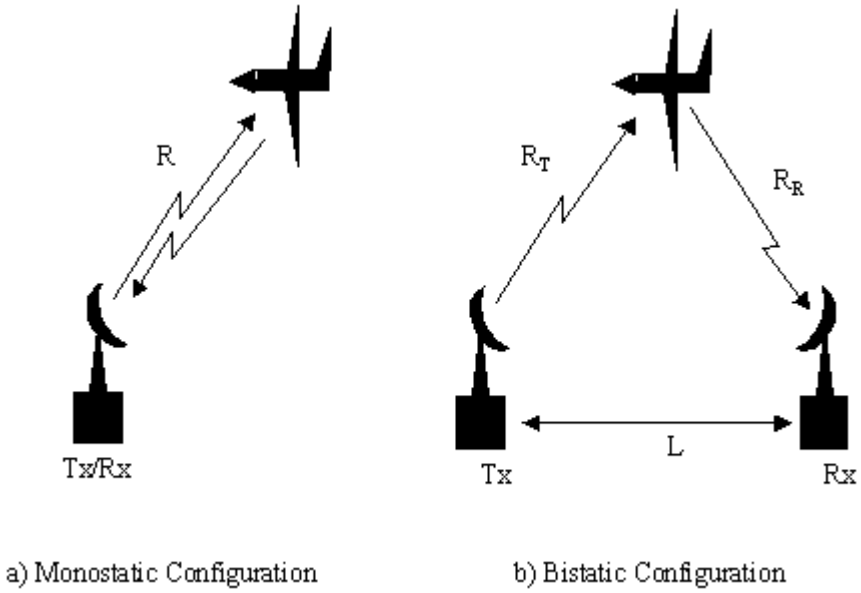

Figure 2.1 Monostatic and Bistatic configurations.

One of the simplest forms of the radar equation, given by Skolnik [11:1.6] is:

$$P_r = \frac{P_T G_t}{4\pi R^2} \times \frac{\sigma}{4\pi R^2} \times A_e \tag{2.1}$$

where:

P_r = Received signal power,

P_T = Transmitter power,

G_t = Transmitter antenna power gain,

R = Range to the object,

σ = Object radar-cross-section,

A_e = Effective aperture area of the receiver antenna.

The left side of equation (2.1), P_r, represents the received signal power as a function of the transmitter and object parameters. The first term of the right-hand side is the radiated power density at range R, i.e., the transmitted power, times the transmitter antenna gain spread over the area of a sphere of radius R ($A = 4 \pi R^2$). The second term, similarly, is the power returned to the radar. Finally, the third term A_e is the effective area of the receiver antenna, which intercepts the incoming signal.

In the bistatic case, the receiver antenna is different than the transmitter antenna in the sense that they are no co-located. The antennas will not necessarily have different values for their parameters.

The effective area of the antenna A_e can also be expressed as:

$$A_e = \frac{G_r \lambda^2}{4\pi} \tag{2.2}$$

where:

G_r = Receiver antenna power gain,

λ = wavelength.

In the bistatic case A_e is replaced with (2.2), in equation (2.1). The difference is most obvious in the length of the path between the transmitter to the object and the receiver to the object. In addition, the radar-cross-section σ_M for a monostatic case is different than the radar-cross-section σ_B for a bistatic case. The radar equation for the bistatic case is:

$$P_r = \frac{P_T G_t}{4 \pi R_T^2} \times \frac{\sigma_B}{4\pi R_R^2} \times \frac{G_r \lambda^2}{4\pi} \tag{2.3}$$

The new terms are:

G_r = Receiver antenna power gain,

R_T = Transmitter-to-object range,

R_R = Receiver-to-object range.

σ_B = Bistatic object radar-cross-section.

Under the above terms, the bistatic object radar-cross-section involves a somewhat different concept than the monostatic case. For a bistatic configuration it is defined as the measure of the energy scattered in the direction of the receiver. Its value would depend on the aspect angle of the object and on the angle between the transmitter and receiver with the vertex at the object. The latter is most commonly referred to as bistatic angle and designated by β. In general, there is no exact formula to convert directly or indirectly the value of the radar-cross-section of an object from one configuration to another, although there is a relation that can lead to certain approximations. There are three regions of bistatic radar-cross-section that can be defined: quasi-monostatic, bistatic and forward-scatter.

Within the first region, the bistatic radar-cross-section can be approximated by the monostatic, under the conditions that the object is located in the bisector of the bistatic

angle and the monostatic frequency is lowered by $cos(\beta/2)$. The monostatic frequency is the frequency at which the monostatic radar-cross-section was measured. The quasi-monostatic region is defined for bistatic angles less than 5º [2:145].

The bistatic region is defined between the bistatic angles where the above theorem fails to predict the bistatic radar-cross-section; and where the forward-scatter region starts at nearly 180º [2:147-155]. In the second region, the bistatic value of σ_B diminishes with respect to the value of σ_M. Unfortunately, this divergence does not vary uniformly.

The third region is defined for high values of β, i.e., values near and up to 180º. Here the value of σ_B should be expected to increase due to Babinet's principle. In simple terms, when applied to the situation where an object is flying between the transmitter and receiver, the principle can be explained as if the physical area of the object represents a slot of the same area on a flat and infinitely thin screen. What the receiver *sees* is a power proportional to $4 \cdot \pi \cdot A^2/\lambda^2$, where A is the area of the slot, and λ is the wavelength. This last parameter should be small compared with the object dimensions [2:150-155].

In equation (2.3), one can also replace P_r with the minimum detectable signal power S_{MIN}, which can also be expressed as:

$$P_r = S_{MIN} = k\, T_0\, B_n\, F_n \left(\frac{S}{N} \right)_{MIN} \tag{2.4}$$

where:

k = Boltzmann's constant (1.38×10^{-23}),

T_0 = Reference temperature to measure the noise figure F_n (290ºK).

B_n = Receiver noise bandwidth,

S/N = Power signal-to-noise ratio.

The factor $T_0 \cdot F_n$ can also be replaced by T_s, the system noise temperature. If equation (2.4) is used to replace P_r in (2.3), and the pattern propagation factors along with the system losses are included, the final result can be solved for the range terms. The resultant expression will be in the exact form presented by Willis [2:68] as a starting point for the analysis of the range equation for bistatic radar, i.e.,

$$\left(R_T R_R\right)_{MAX} = \left[\frac{P_T G_T G_R \lambda^2 \sigma_B F_T^2 F_R^2}{(4\pi)^3 k T_S B_n (S/N)_{min} L_T L_R}\right]^{\frac{1}{2}}. \tag{2.5}$$

Here the new terms are:

F_T = Pattern propagation factor for the transmitter-to-object path,

F_R = Pattern propagation factor for receiver-to-object path,

L_T = Transmitting system losses (not included before),

L_R = Receiving system losses (not included before).

The factor F_T is defined as "the ratio, at the target position, of the field strength **E** to that which would exist at the same distance from the radar in free space and in the antenna beam maximum-gain direction E_0. The factor F_R is analogously defined" [11:2.4]. These two factors include, in the radar equation, the losses suffered due to propagation effects such as multipath, atmospheric absorption and diffraction, and when the object is outside the main beam of the antennas. In other words, when the scenario describes a free-space propagation environment, which is not the case for this research, and the object is located in both antennas' main beam, $F_T = F_R = 1$.

These parameters can also be expressed as $F_T = F_T^{'} \cdot f_T(\theta)$ and $F_R = F_R^{'} \cdot f_R(\theta)$, where $F_T^{'}$ and $F_R^{'}$ are the propagation factor and, $f_T(\theta)$ and $f_R(\theta)$ are the antenna pattern factors. The argument θ is the angle, in the vertical plane, relative to zero elevation.

2.2.3 The Bistatic Geometry. One of the key points to a better understanding of the radar theory for a bistatic configuration is to have a clear picture of the coordinate system and the relations that can be obtained from the geometry formed by the elements involved.

The coordinate system and bistatic plane (the plane formed by the transmitter, the receiver and the object) is depicted in Figure 2.2:

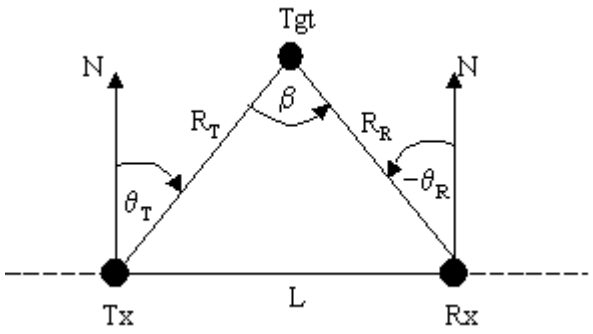

Figure 2.2 North-referenced coordinate system.

The terms θ_T and θ_R are the angles of the transmitter to the object, and the receiver to the object, respectively. Their value is positive when measured clockwise from a North reference axis. When the values of these angles lie simultaneously between –90º and +90º, the object will be in the northern hemisphere. “In general, bistatic radar operation and performance in the northern and southern hemispheres are equivalent for symmetric

geometries"[2:59]. Exception to this includes differences in the terrain, the antenna pattern, radar-cross-section, etc.

As stated previously, β is the bistatic angle and L is the distance from the transmitter to the receiver (also called baseline).

A practical approach to determine the location of the receiver is to define the geometric region where the signal-to-noise ratio (SNR) is adequate for the receiver to perform its processes accurately.

In the triangle of Figure 2.2 formed by the transmitter, the receiver, and the object, if the product of the values of R_T and R_R is set equal to a constant, the geometric space defined by the object is known as the *oval of Cassini*.

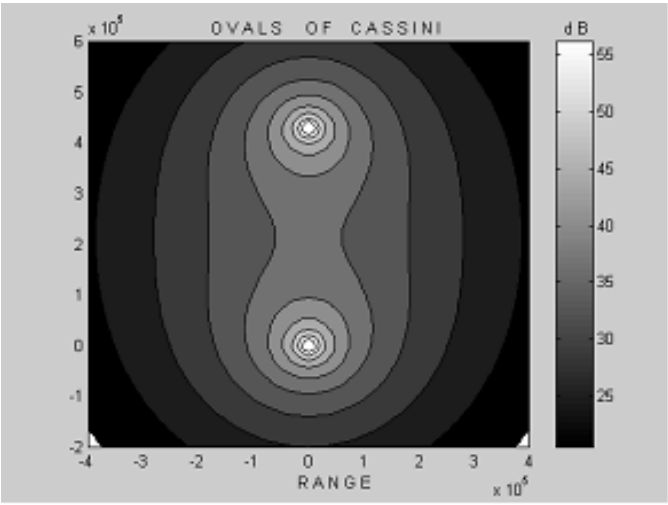

Figure 2.3 Ovals of Cassini.

These ovals, depicted in figure 2.3, provide contours of equal power returned to the bistatic receiver. Note that the region between the transmitter and receiver is one of high sensitivity. Taking into account the convenience of the ovals of Cassini as contours of

constant signal-to-noise ratio, the range equation can be solved for the (S/N) term. Note that the sub index *min* is intentionally omitted from the $(S/N)_{min}$ term so the calculations can show a wider range of levels of available power. The values for the parameters P_T, G_T, G_R, λ, σ_B, F_T, F_R, T_S, B_n, L_T, and L_R are assumed to be known, and their actual value will be discussed later. Then the radar equation is simplified as:

$$(S/N) = \frac{K}{R_T^2 \cdot R_R^2} \tag{2.6}$$

where K = squared right-hand side of equation (2.5), multiplied by (S/N).

Also, the next two relations, obtained from the geometric layout of a bistatic system as in Figure (2.2), will prove to be useful in the foregoing chapters. Their deduction and derivation can be found in chapters three through seven and appendices B through F in [2]. The first one presents the relation between the bistatic angle and the angles defined by the bearing of the object with respect to the north axis when passing through the transmitter, and with respect to the north axis when passing through the receiver. This relation is stated as:

$$\beta = \theta_T - \theta_R . \tag{2.7}$$

The second relation states the value of the bistatic Doppler shift of the carrier caused by the motion of the object. The effect is sensed at the receiver location and, as in the

monostatic case, is caused by the variation in time of the path length of the signal. Its value can be calculated using [2:120]:

$$f_B = (2V/\lambda) \cdot \cos(\delta) \cdot \cos(\beta/2) \tag{2.8}$$

where:

V = Velocity of the object,

λ = Wavelength,

β = Bistatic bisector,

δ = Angle formed by the velocity vector projected onto the bistatic plane and the bistatic bisector ($\beta/2$).

The value of δ is positive when measured clockwise from the bistatic bisector.

2.3 Advanced Refractive Effects Prediction System (AREPS)

To solve the geometry of bistatic radar, i.e., the location of the receiver with respect to the transmitter, one relevant characteristic, among others, needs to be considered. In order to have detection capability, the object needs to be within line of sight of the transmitter and the receiver, and the receiver needs to be located where the scattered signal, from the object, has enough energy to be detected [2:105].

The first step to begin solving the problem of the location of the receiver is to calculate the propagation loss suffered by the electromagnetic waves generated by the television transmitter. This information will be obtained using the "Advance Propagation Model"

(APM) [3]. This model is used by the "Advanced Refractive Effects Prediction System" (AREPS) software [4].

AREPS is a software package that runs under a windows environment to provide signal losses versus range at selected azimuth angles considering the effects of terrain and the atmospheric conditions.

The self-contained APM tool is a range-dependent true hybrid model that divides the troposphere into four regions: the *Flat Earth* region, the *Ray Optics* region, the *Parabolic Equation* region and the *Extended Optics* region.

When using AREPS, the internal development and the mathematical formulation of the algorithms employed to obtain the values of losses, is transparent to the user. Nevertheless, it is of great importance to have a clear understanding of the process involved in order to identify the phenomena of the propagation of the electromagnetic waves.

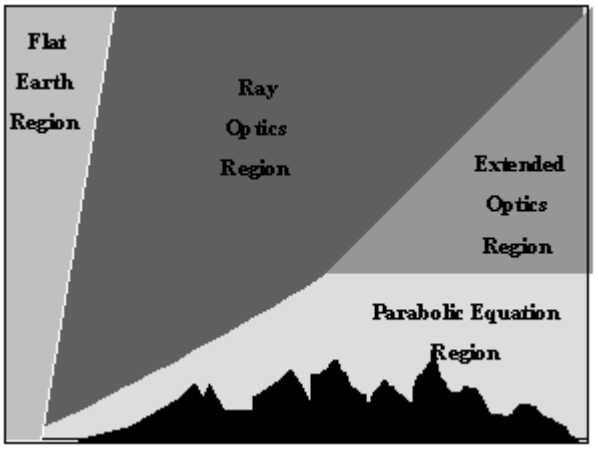

Figure 2.4 APM calculations regions.

2.3.1 Flat Earth Ray Optics Region. The *Flat Earth* model is used to calculate the propagation loss within, approximately, the first 2.5 kilometers from the source of the

electromagnetic waves, i.e. the transmitter. This is done by using a Ray Optics technique and assuming a flat Earth [6:3].

2.3.2 The Ray Optics Region. In this region, the Ray Optics method calculates the propagation loss, accounting for the mutual interference between the direct path and the ray that is reflected on the surface, considering the "refractivity profile at zero range"[6:3]. It also considers focusing and the phase difference due to the different path lengths between the direct and reflected ray. The model gives "precise phase differences and, hence, accurate coherent sums for the computation of propagation loss."[6:3].

2.3.3 The Parabolic Equation Region. The third region, into which the atmospheric volume is divided, uses the *parabolic equation* approach to calculate the loss due to propagation. This model assumes that "the atmosphere vary in range and height only, making the field equations independent of azimuth."[7:90]

This method models the propagation of the electromagnetic wave through the troposphere. The mathematical derivation is fully described in [7, 8 and 9]; following is a brief summary.

The starting point is to define the geometry of a spherical Earth of radius a_e. The source will be located at a height $r = r_s \geq a_e$ and at an angle $\theta = 0$, i.e., on the extension of the radius above the earth. The receiver or probing point will be located somewhere in the far field of the source. The model can be described similarly for horizontal or vertical polarization with the proper substitutions. In this case, the polarization to be used is horizontal.

Once the geometry has been established, the Maxwell's curl equations for the **E** and **H** fields are combined to obtain a vector wave equation for **H**, assuming a source free region ($\mathbf{J}_i=\mathbf{M}_i=q_{ve}=q_{vm}=0$)[1], and a time dependence of $exp(-j\omega t)$, as shown in equation (2.9).

$$\nabla \mathrm{X} \nabla \mathrm{X} \mathbf{H} - \frac{\nabla \varepsilon}{\varepsilon} \mathrm{X} \mathbf{H} - \mu\varepsilon\omega^2 \mathbf{H} = 0 . \tag{2.9}$$

The expression for **H** is expanded in spherical coordinates. For the horizontal polarization case, Hr, H_θ and E_ϕ are the nonzero field components, then $H=H_\phi \hat{\phi}$. Next, the scalar wave equation is obtained in the form [8:382]:

$$\frac{1}{r}\frac{\partial^2}{\partial r^2}\left(rE_\phi\right)+\frac{1}{r^2}\frac{\partial}{\partial\theta}\left[\frac{1}{\sin(\theta)}\frac{\partial}{\partial\theta}\left(\sin(\theta)H\phi\right)\right]+\mu\varepsilon\omega^2 E_\phi = 0 . \tag{2.10}$$

For the above expression, ω is the angular frequency. The magnetic permeability μ is assumed to be constant. The electric permitivity ε varies slowly enough in the ϕ direction to ignore all the components in that direction, with ϕ being the angle on the X-Y plane.

Once equation (2.10) is obtained, a substitution is made to replace H_ϕ in order to obtain a simpler wave equation. In addition, a transformation to the rectangular coordinate system is performed. The X-axis will be the earth's surface with the origin at the base of the source. These two actions plus the approximation [8:384, 9:1465]

[1] $\mathbf{J}_i$ and $\mathbf{M}_i$ are the electric and magnetic current density, respectively. q_{ve} and q_{vm} represents the electric and magnetic charge density correspondingly.

$$k \left| \frac{\partial \psi (x, z)}{\partial x} \right| \rangle\rangle \left| \frac{\partial^2 \psi (x, z)}{\partial x^2} \right| \tag{2.11}$$

will lead to the formulation of the parabolic wave equation for a flat earth [7:92], expressed as:

$$\left(\frac{\partial^2}{\partial z^2} + 2ik_0 \frac{\partial}{\partial x} + k_0^2 \left[n^2(x,z) - 1 \right] \right) \psi(x,z) = 0 \tag{2.12}$$

where

$\psi(x,z)$ = Scalar component of the electric field,

x = Range,

z = Height in Cartesian coordinates,

k_0 = Free space wavenumber ($k_0 = \omega / c$),

n = Index of refraction ($n = \mu\varepsilon / \mu_0\varepsilon_0)^{1/2}$ where μ_0 and ε_0 are the vacuum values of μ and ε.

When appropriate boundary conditions are set to $z = 0$ and $z = \infty$, this differential equation can be solved using the Fourier split-step algorithm also described in [7, 8, 9]. "This method is based on the fact that the Fourier transform of (2.11) has a simple solution at $x + \Delta x$, in terms of the solution at x, provided the refractive index can be considered locally constant in x and z" [9:1465].

A change of variable is performed where the height of the terrain is expressed as a function of the range ($\zeta = z - T(x)$), and where $T(x)$ is the function that describes the

height of the terrain at the different values of the range. From the substitutions, transforms and derivations detailed in [7], equation (2.12) becomes the split-step parabolic equation algorithm [7:91] given by:

$$\psi(x+\Delta x,\zeta)=e^{jk_0\Delta x\left[10^{-6}M(\zeta)-\zeta t''(x)\right]}\Im^{-1}\cdot\left\{e^{j\Delta x\left(\sqrt{k_0^2-p^2}-k_0\right)}\Im\{\psi(x,\zeta)\}\right\} \qquad (2.13)$$

where:

x = Range,

$M(\zeta)$ = Modified refractivity unit ($[n-1+\zeta/a]\cdot 10^6$), which would characterize the effects of refraction over a flat earth[2].

a = Earth's radius,

$t''(x)$ = Second derivative with respect to x,

$p = k_0 \sin(\theta)$ which is a transform variable, function of the propagation angle θ,

θ = Angle relative to the horizontal.

$\Im$ = Fourier transform,

$\Im^{-1}$ = Inverse Fourier transform.

The field $\psi(x+\Delta x,\zeta)$ represents the field propagated from x, obtained from the resultant field at the boundary of the optical region, to Δx in free space (second term of (2.13)), and attenuated by the environment (first term of (2.13)).

[2] The use of the value of n will represent the waves in a somehow straight line between two points over a curved earth. On the other hand the use of M will represent the propagation of the waves in an upward bending line over a flat earth.

One of the benefits of this process is that since the algorithm uses a recursive method to determine the field, one can obtain the losses at any desired range and at any specific azimuth, allowing the user to build a coverage diagram. It has been shown in [7:93-97, 8:389] that the model described above provides excellent agreement of its results with real data.

2.3.4 The Extended Optics Region. This region is located above the Parabolic Equation Region, and is calculated using ray optics methods, initialized with the results from the Parabolic Equation.

The aforementioned methods obtain the data from the input given by the user in the form of two files containing the atmospheric refractivity and the terrain elevation data. The other input needed are the parameters of the transmitter.

In terms of the accuracy of this model there are some comparisons of its predictions with the real data shown in [7]. The values of the prediction compared to those of the measured data "where shown to give predominantly excellent agreement"[7:98]. Also, in an e-mail written on November 26, 2001, by the author of [7], and currently working with the producers of [3] and [4], stated that: "There have been a few reports by independent organizations showing comparisons of AREPS with real measurements which have shown good agreement (although these are not published)".

2.4 Refraction

As shown in the last equation, AREPS considers for the loss predictions, mainly the effects of the terrain height and the refractivity index. This section will cover the theory behind this concept.

When an electromagnetic wave propagates through the lower part of the atmosphere, namely, the troposphere, it is affected by such factors as absorption, scattering, and bending. This thesis focuses on frequencies in the range of VHF (30 MH_Z to 300 MH_Z), for which absorption is not a problem. [10:6.19]

The fact that the waves are bent is due to the phenomena of refraction. The term *refraction* refers to the property of a medium to bend an electromagnetic wave as it passes through the medium. A measure of the amount of refraction is the index of refraction, n. As indicated in [5:23], this concept is defined as the ratio of the velocity of propagation in free space, c, (away from the influence of the earth or other objects) to the velocity in the medium, v. Mathematically, this is

$$n = \frac{c}{v} \ . \tag{2.14}$$

The normal value of the refractive index, n, for the atmosphere near the earth's surface varies between 1.000250 and 1.000400. For a study of propagation, the index of refraction is not a very convenient number. Therefore a scaled index of refraction, N, called refractivity, has been defined. At microwave frequencies and below, the relationship

between the index of refraction n and refractivity N, for air that contains water vapor is given in [10:6.20] as

$$N = 77.6 \cdot \frac{P}{T} + 3.73 \times 10^5 \frac{e}{T^2} \tag{2.15}$$

where

P = Atmosphere's barometric pressure in millibars,

e = Water vapor pressure in millibars,

T = Atmosphere's absolute temperature in Kelvin.

Thus, the atmospheric refractivity near the earth's surface would normally vary between 250 and 400 *N-units*. Since the barometric pressure and water vapor content of the atmosphere decrease rapidly with height, while the temperature slowly decreases with height, the index of refraction, and therefore refractivity, normally decreases with increasing altitude.

As a tool in examining refractive gradients and their effect upon propagation, a modified refractivity, defined as $M = N + 0.157h$ for an altitude h in meters is often used in place of the refractivity. There are several conditions that may be encountered on the earth's troposphere. The following are the more relevant and are described according to [5:25-31].

In practical terms, when the gradient[3] of $N = -39$ *N-units* per kilometer, normal propagation takes place. For values of *dN/dh* less than –39 *N-units* per kilometer, the radio wave is bent strongly downward. This phenomenon is called subrefraction.

Even though the refractivity distribution decreases exponentially with height, this variation is sufficiently regular to use a linear function as an approximation. "This function is known as a *standard* gradient and is characterized by a decrease of 39 *N-units* per kilometer or an increase of 118 *M-units* per kilometer"[5:25]. As stated previously, a *standard* gradient will cause the traveling waves to bend downward from a straight line. A *normal* gradient is one that causes a similar effect but the values vary between 0 and -79 *N-units* per kilometer or between 79 and 157 *M-units* per kilometer.

When *dN/dh* is less than –157 *N-units* per kilometer, the radio wave can be bent downward sufficiently enough to be reflected from the earth, after which the ray is again bent towards the earth, and so on [10:6.20]. This refractive condition is called *trapping* because the wave is confined to a narrow region of the troposphere.

A less dramatic bending occurs when a temperature inversion occurs. In other words, when the temperature increases with height and/or the amount of water vapor on the atmosphere decreases rapidly with height. Under these circumstances the refractivity gradient will decrease from the *standard*. The propagating wave will be bent downward from a straight line more than normal. This type of refraction is known as superrefraction.

Other phenomena on the atmospheric behavior with respect to electromagnetic wave propagation are the formation of ducts. A duct is a channel in which electromagnetic

[3] The gradient *dN/dh* is the rate of change in refractivity with respect to height h.

energy can propagate over great ranges. The thicker the duct, the lower the frequency that can be propagated inside of it.

All of the above plus other phenomena detailed in [5], affect the amount of signal losses on the transmitter-to-object and receiver-to-object path. Therefore, they represent an aspect to be considered in the analysis of simulation outputs to determine whether signal levels are the result of a special propagation condition, or a scenario expected to be found most of the time.

Some of the effects described above are depicted in Figure 2.5.

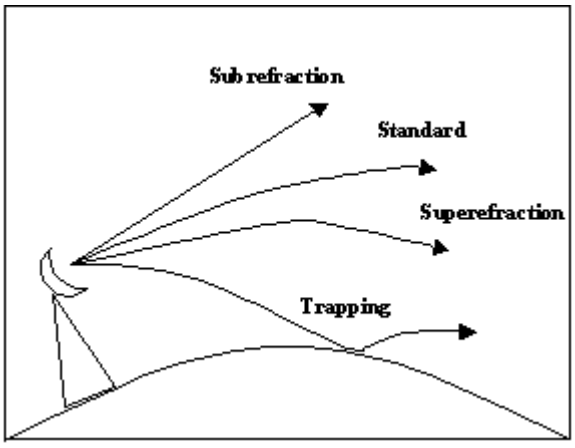

Figure 2.5 Refractive conditions [5:25].

2.5 Meteorological Data

The meteorological data contains the necessary information for AREPS to calculate the refractive gradients and determine the condition of the troposphere (trapping, super-refraction, normal, standard, or sub-refraction). This information can be used to determine

the propagation loss. The format of the data is arranged in columns. Data such as the altitude at which the measurement was performed, the barometric pressure in millibars at that height, the water vapor pressure in millibars, and the atmosphere's absolute temperature in Kelvin can be found. The data can be obtained from the World Meteorological Organization website as a ftp file, or from any website containing this information.

2.6 Digital Terrain Characterization

The terrain is a factor that plays one of the most significant roles in the analysis performed to optimally place a monostatic radar. Because of the requirement for line-of-sight with the object, these systems are normally located on the highest elevations of the terrain. On military applications they may look for a position that enhances the coverage toward a specific sector. For the bistatic case the analysis is more challenging since there is not one but two sites that need to have line-of-sight with the object. In addition, the transmitter is fixed and cannot be moved. The concept of the system is to hitchhike from a source that is part of a given scenario.

For this research, the terrain is simulated by a collection of values representing geographical heights in a predefined region. Those values define a well behaved topography, meaning that there will be valleys and mountain ranges that run exactly parallel to each other. At the same time, the terrain is intended to fit within the category of irregular or mountainous. These characteristics provide extreme detection conditions in the sense that there are areas where the transmitter signal does not reach, but the receiver has perfect line-of-sight, and vice versa, or where for both elements the line-of-sight is

marginal. At the same time it is possible to roughly estimate potential receiver locations to allow checking the radar equation solution obtained after the calculations and determine if it represents a valid answer. Finally, this method of generating terrain data can be used to define any desired topography with very specific requirements such as elevation, resolution, roughness, etc. An example of the above can be observed on Figure 2.6.

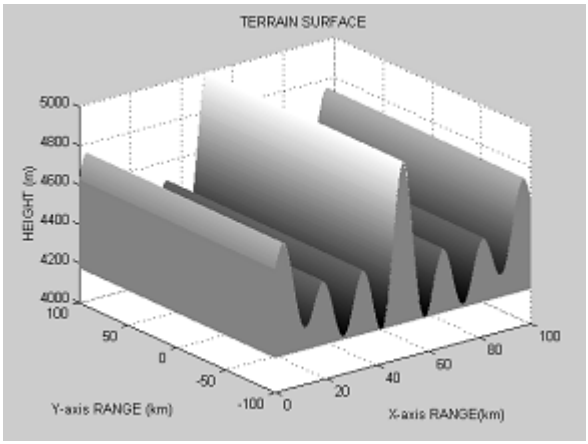

Figure 2.6 Digital Terrain Characterization.

The structure of the file containing the elevation data must comply with the specifications required by AREPS. As mentioned before, the input necessary for the software to predict the propagation losses are terrain, atmospheric conditions and transmitter and receiver parameters.

AREPS accepts two types of terrain. The first kind is in the format of *Digital Terrain Elevation Data* or *DTED*. In simple terms, a *DTED* file contains the elevation data of an explicit grid, limited by earth coordinates in a particular format. There are three different resolution levels available: 0, 1, and 2. The level 0 format is the lowest horizontal resolution, giving height information every 30 arcs per second (approximately 1000

meters). Level 1 format has a horizontal resolution of 3 arcs per second (approximately 100 meters). Finally, the level 2 format has the highest horizontal resolution of 1 arc per second (approximately 30 meters). This information is provided by the National Imagery and Mapping Agency (NIMA), and the *DTED* level 0 files have unlimited distribution and can be downloaded for free from its website.

The second type of terrain input to AREPS is called *My Own Terrain*. This is the mode of operation that lets the user define a customized terrain just like the one described above. The terrain information consists in a column vector containing the range steps from an explicit coordinate, and a column vector containing the height at those range steps. They can be entered manually or as a file. The later is the case for this research. The file must be in ASCII format, having in the first column the range values, and in the second column the corresponding height values. AREPS does not impose a limitation on the amount of range steps, its values, or height values. The only constraint is that the first range value must be zero. This is because in *My Own Terrain* mode the landscape is defined from the center of the grid. All the calculations and the initialization of the algorithms assume that the source of the electromagnetic waves is on the center of the terrain. Therefore, it is necessary to include the bearing at which the specific terrain profile is defined. In other words, the bearing is the azimuth along which the terrain data applies. This value is entered as a whole number. As can be expected, it is necessary to calculate the previously mentioned vectors and construct a corresponding file for every single bearing needed. Furthermore, if it is necessary to predict the losses of a signal coming from a source located in a point not centered on the terrain, it is necessary to come up with a different formula to calculate the needed vectors. These procedures will be detailed in Chapter III.

The generation of the Digital Terrain Characterization is performed in Matlab® using known mathematical functions, and evaluated with arbitrary parameters to obtain a topography with the desirable features described before.

2.7 Transmitter Parameters

In a PCL system the transmitter parameters are a given. Its effective radiated power, frequency, modulation, location, etc., cannot be changed. Therefore the coverage, the resolution and the overall performance of the radar system will depend entirely on the receiver location and the signal processing. Fortunately, for obvious commercial reasons, most of the broadcast transmitters (TV and radio stations) use omnidirectional antennas to reach the widest possible area at ground level.

Since the general research objective is to determine the best location for the receiver, particular values and parameters are defined, but the ever-changing technologies have and will alter some ways of implementing the passive system under consideration. For example, TV and radio transmitters will soon start operating under the *new* standards of the Digital Audio Broadcasting (DAB) and Digital Video Broadcasting (DVB). Furthermore, there are already experiments being performed exploiting transmitters using these types of signal. As a result, the receiver location problem will be treated as a general problem in terms of the type of signal being transmitted, but as a particular problem in the calculations to be performed. As established in the first chapter, the purpose of this research is stated broadly in terms of the source type.

In this case, the model is constructed using an analog TV station operating at 200 MHz. This frequency is beneficial in the sense that it is not severely affected by rain,

snow, or fog; in some cases, due to diffraction, makes possible detection beyond line-of-sight. The modulation is AM Vestigial Side Band. The Output Power of the visual transmitter[4] is set to 50 kW. The antenna is approximated as omnidirectional with a 8 dB gain (and therefore with a gain of 0 dBi), horizontally polarized and located 50 meters above the ground. These values correspond to an Effective Radiated Power (ERP) of approximately 316 kW. The previous data represents possible real values for a broadcast station operating in channel 8 [10:7.3]. This value implies the power of the whole signal. Due to the modulation scheme, the total carrier power will be approximately 50% of the total power [1:21]. Therefore, the power value to be used in the bistatic radar equation *Pt* will be 158 kW.

In general, analog TV transmitters radiate a strong carrier frequency, which easily allows for detection of moving objects, and makes it possible to perform angular measurements. The problem is that, due to the modulation type used, the range estimates are rough; but for detection and early warning applications, they represent a useful source [12:4].

2.8 Receiver Parameters

In these forms of passive radar systems the parameters of the receiver, such as antenna, bandwidth, noise temperature, etc., determine how far it can be placed from the transmitter and the object at the same time, considering only the available signal-to-noise ratio relationship and the given transmitter and object parameters. A quick look at equation (2.5) and (2.6) will tell us that the smaller maximum range product $R_T \bullet R_R$ will be obtained from

[4] The transmitter which processes the video signal

the minimum possible value of the signal-to-noise ratio that the receiver can handle; a parameter of the noise temperature and noise bandwidth. The maximum of the above product will also be a factor of the antenna gain used on the receiver.

As said previously, for simulation purposes, the following values will be used for calculations. The noise temperature will be set to 500 ºK and the noise bandwidth to 0.5 Hz. Assuming a required signal-to-noise ratio for detection of 24.62 dB (chosen to round the value of the final result) and ignoring the losses of the system, from equation (2.4), the detection threshold will be -180 dBW given by:

$$S_{MIN} = 10 \cdot \log_{10}\left(1.38 \cdot 10^{-23} \cdot 500 \cdot 0.5\right) + 24.62 = -180\text{dBW} \tag{2.16}$$

The antenna parameters will be arbitrary. The system will hypothetically use a linear phased array antenna[5] consisting of 16 elements horizontally polarized. Its configuration will allow DOA (only in azimuth, since this is a linear array) and Doppler shift measurements. The maximum gain at boresight will be 15.45 dB, the 3dB beamwidth will be 8º.

The original simulation output for the pattern was symmetric with respect to the [–90º; 90º] reference axis. For this research, it was assumed that an infinite Perfect Electric Conductor (PEC) was placed behind the elements. Given that it is not the intention of this research to perform a complete antenna analysis, the following rough approximation is performed. The effect of the PEC, using image theory [14:63-65, 15:164-165], implies the

[5] The antenna characteristics are the result of the simulation performed on NecWin Plus+ by AFIT MSEE student (2002) 1st Lt. (Turkish Air Force) Baris Calikoglu, for his thesis research "Analysis and Evaluation of Array Antennas for PCL Systems".

cancellation of the back lobes. In addition, the gain on the front lobes will be increased approximately by 3 dB. This procedure is performed to eliminate the back lobes. Regarding this operation, it is important to keep in mind that all the parameters used in the calculations, including the terrain and the transmitter and receiver hardware, are only a representation and do not describe any particular values or trends gathered on any specific equipment or environment. Therefore, the antenna pattern described is only a reference. The calculation methodology of the loss values of the direct and indirect signal affected by this antenna pattern applies for any other simulated or real one. The resulting antenna pattern will be as the one shown in Figure 2.7.

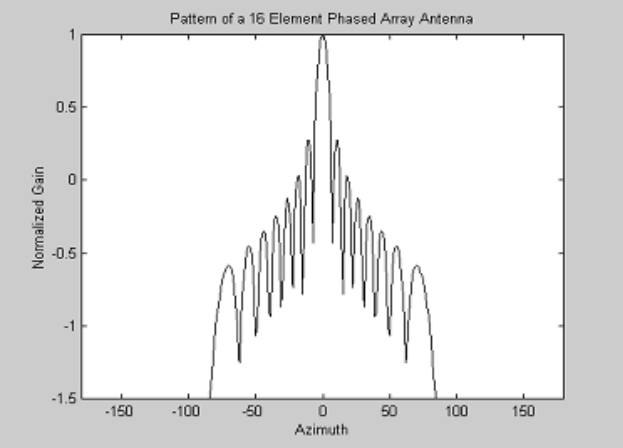

Figure 2.7 Receiver Antenna Pattern.

The antenna height h_a initially will be set at approximately 20 meters above the ground to avoid elevation lobbing [1:79].

The use of phased-array antennas and digital beam forming will obviously increase the flexibility and performance of the system, specifically for estimation of azimuth, due to the possibility of dealing with the positions of the main lobes and the nulls. Once again, the

information needed to perform the calculations is based only on the figures of merit of the antenna and not on the specific type.

The receiver needs to obtain a reference signal from the transmitter other than the scattered signal from the object to have a reference to compare the phase of the scattered signal from an object. This is where the word *coherent* fits in PCL. This signal must be strong enough to activate the receiver, but it cannot cause the receiver to saturate or to *cover* the signal from the object. Doppler and/or spatial filtering (place a null in the direction of the transmitter) must be performed to avoid this condition. The effects of the direct signal over the returned echo from the object, before and after filtering, can be observed on the experiments presented on [12] and [13], as seen in Figure 2.8.

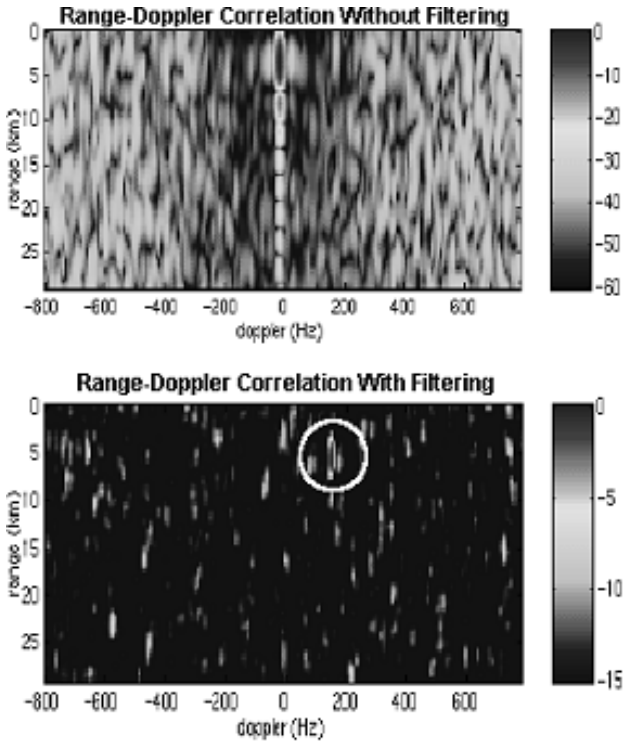

Figure 2.8 Effects of the direct signal on the receiver before and after filtering [13:8].

2.9 Object Parameters

The object influence on the PCL problem is represented in the denominator of equation (2.5). For this research, the bistatic radar-cross-section is non-fluctuating with a value of $10m^2$. Nevertheless, in the analysis of the results (Chapter IV), this factor is included in a more realistic sense, considering its changes depending on the object position with respect to the transmitter and the receiver.

2.10 Summary

This chapter sets the foundation of the problem of a PCL system in terms of the geometry and when propagation losses, due to the atmospheric conditions and the terrain, are considered. The AREPS software, based on the parabolic equation, helps to determine the values of these losses, considering the terrain and the local atmospheric factors. These losses will allow establishment of a pattern of signal loss levels, which when combined with the bistatic radar equations makes it possible to determine the signal power level on every coordinate of a given terrain. This condition is key to a more realistic analysis of a Passive Coherent Location system.

III. Methodology

3.1 Introduction

This chapter systematically details the steps to be followed in order to determine the best location for the receiver (s) with respect to the transmitter.

After detailing the terrain to be used, the general scenario will be defined, the location of the transmitter and the more relevant areas where detection should be focused will be addressed, and the simulated terrain files to be used on the software packages will be generated. The signal levels will be calculated at every point where the receiver antenna can be located. These signals are the direct signal and that from the object. Once these calculations are performed, the total signal level will be established for further analysis (next Chapter).

3.2 General scenario

3.2.1 The Terrain. Simulated terrain is generated using arbitrary functions to obtain the desired characteristics. Its physical area will be defined by a square of 200 Km by 200Km. As shown in Figure 3.1, the reference system has its origin at the center of the square, where the positive Y-axis represents the North, or 0º bearing, and the positive X-axis is the 90º bearing. The quadrant identification is the same as normally used in trigonometry; from I to IV, counterclockwise, starting from the one defined by the positive X-axis and the positive Y-axis.

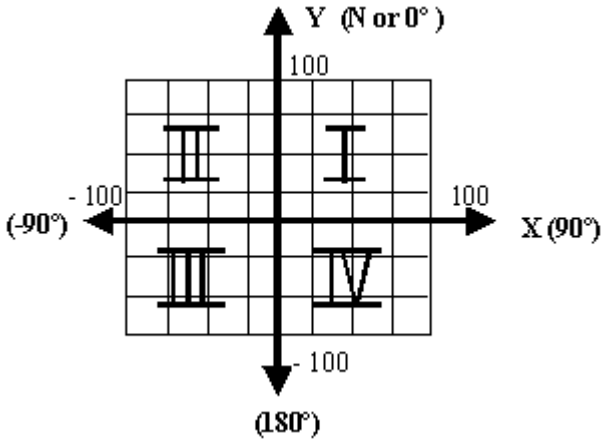

Figure 3.1 Grid and coordinate system, including the quadrant identifiers.

Using Matlab®[1], the starting point is to define two equal vectors **x** and **y**, on the interval [-100 100], in order to generate a square grid of 201 by 201 at steps of 1 unit.

Then, a terrain profile is generated by selecting and evaluating a mathematical expression for the values defined on the grid. The goal is to create a terrain symmetric with respect to both, the X-axis and the Y-axis, where the terrain elevation for a given value of **x** is constant, for all values of **y**. The maximum height will be at $\mathbf{x}_{101} = 0$. In other words, the general objective is to generate a terrain profile where the highest elevation is at the center of the grid, along the Y-axis, and a set of valleys symmetrically distributed at each side of it.

The particular terrain generating function, which defines the height z at every coordinate within the first and fourth quadrant, is given by:

[1] Matlab® is the software used for mathematical simulation throughout this thesis. Other simulation software such as Mathcad® or Mathematica® may be useful as well.

$$Z = 5\times10^{3}\cdot(Y_1 + Y_2 + Y_3 + Y_4 + Y_5 + Y_6) \tag{3.1a}$$

where:

$$Y_1 = \mathrm{sinc}^2(0.1\cdot X) \tag{3.1b}$$

$$Y_2 = 0.9\cdot\mathrm{sinc}^2(0.1\cdot(X - 10\cdot\pi)) \tag{3.1c}$$

$$Y_3 = 0.9\cdot\mathrm{sinc}^2(0.1\cdot(X - 20\cdot\pi)) \tag{3.1d}$$

$$Y_4 = 0.95\cdot\mathrm{sinc}^2(0.1\cdot(X - 30\cdot\pi)) \tag{3.1e}$$

$$Y_5 = 0.9\cdot\mathrm{sinc}^2(0.1\cdot(X - 40\cdot\pi)) \tag{3.1f}$$

$$Y_6 = 0.9\cdot\mathrm{sinc}^2(0.1\cdot(X - 50\cdot\pi)) \tag{3.1g}$$

and:

$$\mathrm{sinc}^2(0.1\cdot X) = (\sin(0.1\cdot X)/(0.1\cdot X))^2\,. \tag{3.1h}$$

The whole terrain grid is obtained by substituting the values **Z** of the second and third quadrant ($\mathbf{Z}_{(1:201,1:100)}$)[2] with the values of **Z** on the first and fourth quadrant ($\mathbf{Z}_{(1:201,102:201)}$) by flipping it left-to-right, and substituting the values at $\mathbf{X}_{(1:201,101)}$) by 5,000. The latter because the *sin(x)/x* function has a value of 0/0 at x=0.

Once equation (3.1a) is evaluated on the intervals defined by **x** and **y**, the resulting surface features a main centered elevation representing a height of 5,000m, three minor peaks at each side of the Y-axis, of 4,500m at (±) 31.5km, 4,499.9m at (±) 63km, and 4,749.8m at (±) 94km. There are also three main valleys. Their elevation and location are:

[2] The notation $\mathbf{M}_{(1:m,1:n)}$ means rows 1 to m, and the columns 1 to n of matrix **M**.

4,179.8m at (±) 17km for the first and deepest valley, 4,196.6m at (±) 47km for the second valley, and 4,295.3m at (±) 76.5km for the third valley (as shown in Figure 3.2).

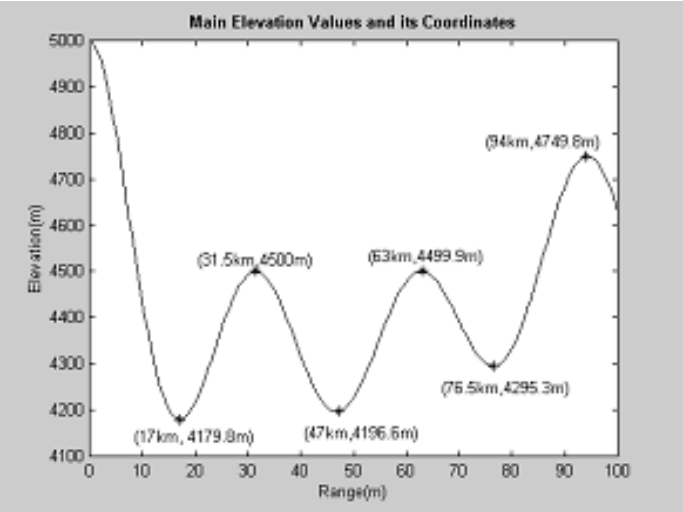

Figure 3.2 Terrain profile at 90º including the main elevation values and its coordinates

The complete terrain surface was shown in Figure 2.6

Up to this point, there are three matrices of 201 by 201 elements each:

– The **X** matrix, containing equal rows, which are the copies of vector **x** (Figure 3.3 a).

– The **Y** matrix, which is the transpose of the **X** matrix, having equal columns which are the copies of vector **x** (Figure 3.3 b).

The **Z** matrix containing the height *z* of the terrain at every coordinate defined by each pair of elements of **X** and **Y** with corresponding indices. As expected, each column has a constant value (Figure 3.3 c).

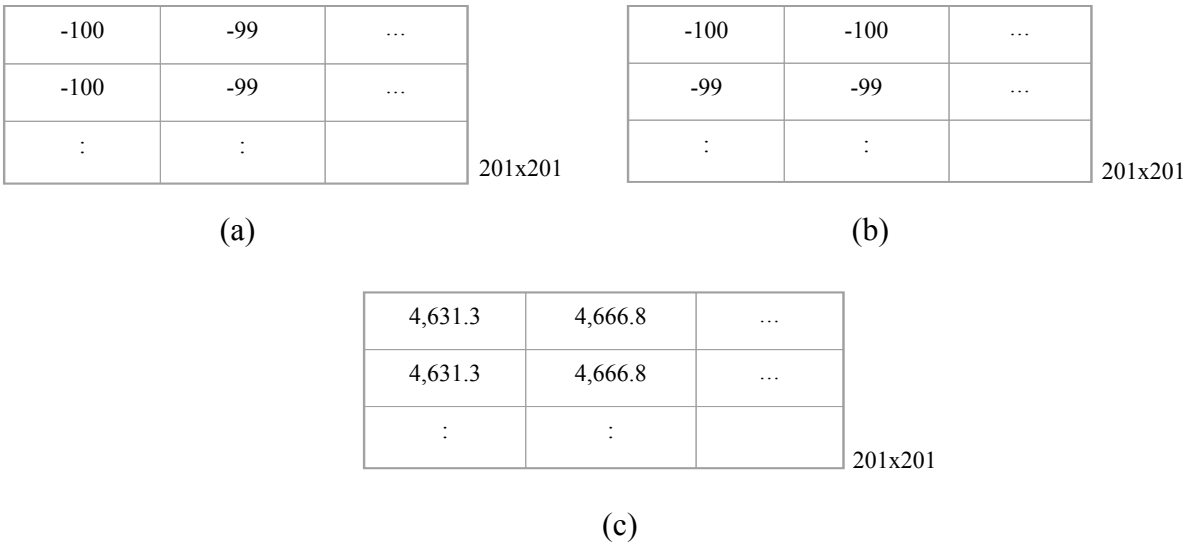

Figure 3.3 Matrices layout. (a) Matrix **X**. (b) Matrix **Y**. (c) Matrix **Z**.

As it was detailed previously, one of the goals is to determine the transmitted signal level at every point in the terrain using AREPS. When using a customized terrain this software requires an input consisting of a terrain file containing the range-height couplets for every single bearing where propagation loss prediction is required.

In order to generate the terrain files for each desired azimuth it is necessary to transform the terrain data into a cylindrical coordinate system format. Where possible the idea is to obtain a set of matrices to discriminate the height elements based on its indices. In other words, the coordinate transformation allows obtaining an angle matrix where the indices of the elements of a desired value define, in a range matrix and a height matrix, the corresponding elements necessary to build the terrain files.

The equations to be used on the coordinate conversion process are:

$$r = \sqrt{x^2 + y^2} \tag{3.2a}$$

$$\tan(\theta) = \frac{y}{x} \tag{3.2b}$$

and

$$z = z \tag{3.2c}$$

The result after the conversion is three matrices **R**, **T**, and **Z**. The ranges from the origin to every coordinate on the grid form the matrix **R**. The matrix **T** contains the angles formed by the range vector with respect to the positive X-axis, ranging from 0º to 180º for points located on the first and second quadrant, and from –1º to –179º for points located on the third and fourth quadrant. Finally, the matrix **Z** will not be altered.

In this step, only the first quadrant is considered on the loss predictions. The reasons are that; the transmitter is located on the origin of the coordinate system; the terrain is symmetric with respect to both axis; and the first calculations to be made are the losses of the signal transmitted by an omnidirectional antenna.

The losses at 19 different azimuth values are calculated within the first quadrant. This is every five degrees, starting at 0º and ending at 90º. This grade of resolution should be more than enough to provide a good reference for the real signal losses. The standard to calculate the coverage of a TV station suggests a loss prediction at 8 radials from the transmitter antenna site [10:6.31].

At this point, it is necessary to decide an approach to use to generate the terrain files for its use on AREPS.

The first option is to generate a row vector **RI**, containing the range values from 0 m to the maximum range available at each of the 19 specific bearings. The length of the vector is given by the range step size selected when building the vector **RI**. A second row vector, **TI**, the same length of **RI**, is generated containing all elements of the same value. This value represents the angle θ_T, with respect to the north reference system shown on figure 2.2. The value of θ_T is 90º minus the value of the desired bearing, since after the transformation to cylindrical coordinates the angle values where measured having as a 0º reference the X-axis. The above transformation is made to be consistent with the selected reference system. An interpolation of the data contained on the matrices **R**, **T**, and **Z** with the values of the vectors **RI** and **TI** is performed to obtain a new vector **ZI**, with the corresponding terrain elevations at the values specified on **RI** and **TI**.

The results obtained with this process were not satisfactory. When plotting the outcomes, only the vectors for 0º and for 90º agreed with the three dimensional terrain. The other vectors were generated with a great amount of *noise*. As an example Figure 3.4 shows the output generated by the Matlab® code written using the method described above.

The second option (used in this thesis) involves obtaining from the **T** matrix the indices [i,j] of the values nearest to the desired bearings, within 0.1º. As in the previous case, this value is 90º minus the value of the desired bearing. Then, from the matrices **R** and **Z** extract the values corresponding to the indices [i,j] and form two new vectors **RI** and **ZI,** respectively.

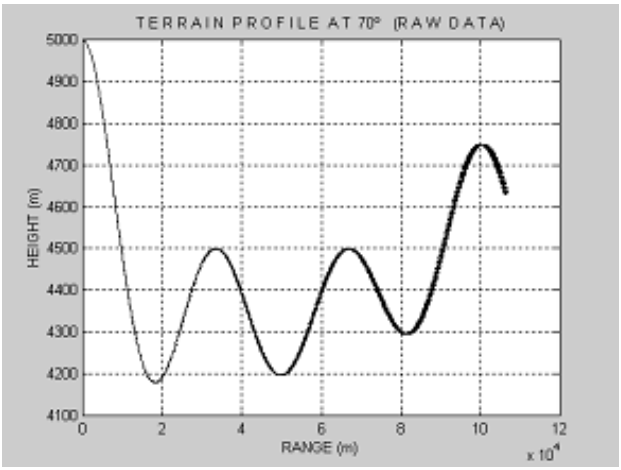

Figure 3.4 Terrain profile generated using interpolation. The noise can be observed at the right of the 40,000 meters mark

This method generates an elevation vector with considerably less *noise*. To clear out the *noise* it is possible to use a polynomial regression and then evaluating the polynomial. This is done automatically in Matlab®. An example of this case is shown in Figure 3.5.

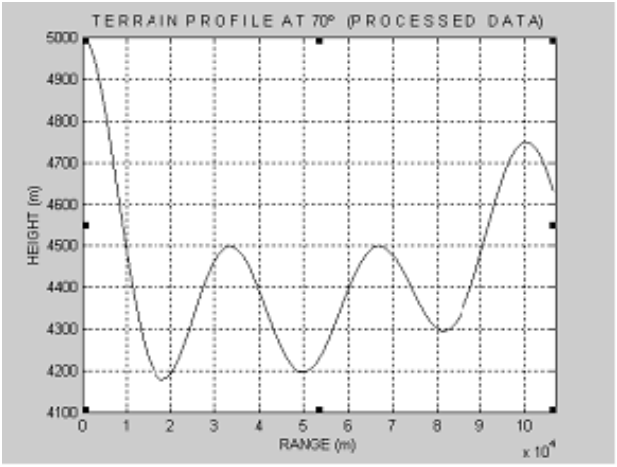

Figure 3.5 Terrain profile using the nearest values to the desired bearing

The resulting vectors for each bearing, which are to be used as terrain files on AREPS, are saved on an ASCII file having as the first column the vector **ZI** and as the second column the vector **RI**. The 19 terrain files are plotted upon of the surface defined in the first quadrant, as shown in Figure 3.6.

Once the 19 vectors are defined and saved, it is possible to go to the second step of the process, i.e., determine the signal level of the transmitter at every point in the terrain.

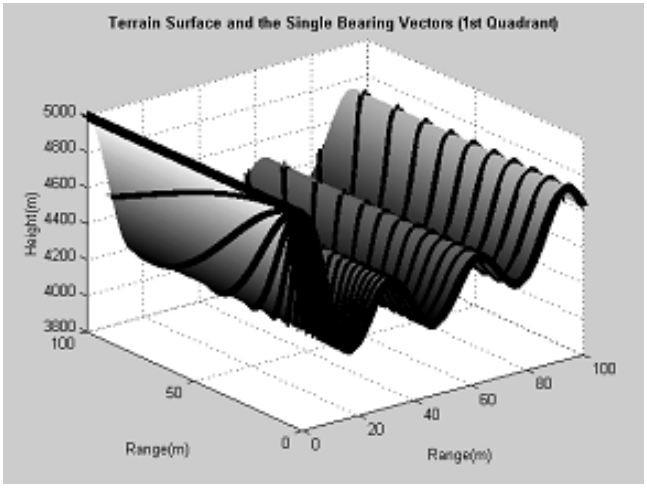

Figure 3.6 Elevation vectors plotted on top of the terrain surface

3.2.2 The Meteorological Conditions. The meteorological data and the atmospheric parameters to be used for the calculations were obtained from the weather station located in Albuquerque, New Mexico on July 06 of 2001. This station was selected for being located in a dry weather region, and the date was an arbitrary summer day. As with the receiver antenna pattern, the meteorological information, simply gives a frame of reference. When processing real terrain and real hardware data, the atmospheric parameters should be

obtained from the closest weather station available. The data can be easily obtained from any site on the Internet containing this type of information[3].

The data is presented in different formats. Two of them are used in this research. One of them is called *Text:List*. It is a list containing the measured parameters, in columns, and at the end the information regarding the station information (location, identifier, observation time), and sounding indices. Here a readable data is presented where a general picture can be visualized.

The other format is the *Text:Raw*. Here the data is presented following the WMO code. It is not easy to read but is the format used by AREPS. To import the data to AREPS it is necessary to select the information, copy it, and paste it on the *New Environment* window of AREPS, on the *Import WMO code* tab. The software automatically calculates and generates a *Propagation Condition Summary* where the propagation conditions are presented and the plots of the *M* and *N* units versus height are displayed. Also a plot showing the *Gradient Ducts* is depicted.

3.2.3 The Transmitter. The transmitter is located at the origin of the simulated terrain, i.e., at (0; 0; 5,000). Its parameters, detailed in Chapter II, are summarized in Table 3.1.

[3] For this research, the source was the website maintained by the University of Wyoming, where there is current and past information from weather stations from all around the world. The website can be found at http://weather.uwyo.edu/upperair/sounding.html.

Table 3.1 Transmitter parameters.

PARAMETER	VALUE
Transmitter Power	158 kW
Frequency	200.00 MHz
Antenna Type	Omnidirectional
Antenna Gain	8 dB
Antenna Polarization	Horizontal
Antenna Height	50 meters above the ground

3.2.4 The Object. On the definition of the general scenario, it is important to determine a main Area of Interest (AOI) from a surveillance point of view. It is assumed that the most likely penetration route for a moving object will be from the North, at the bottom of the deepest valley (very likely to happen), at a flight level, FL, of 100 m above the ground. It is also an assumption that the PCL system only needs to provide early detection at low-level coverage. Therefore, according to the description of the terrain and also shown in Figure 3.2, the object will be for the first time on the grid at the coordinates (17,000; 100,000; 4,279.8) or at the cell (1,118) on the three matrices **R**, **T**, and **Z**, or **X**, **Y**, and **Z**, at a height $z = \mathbf{Z}_{(1,118)} + 100$, considering only the first and fourth quadrant.

3.3 The Transmitter-To-Receiver Path

3.3.1 The Direct Signal Without the Effects of the Receiver Antenna Pattern. Once the general scenario has been established it is possible to start the calculations. The first signal loss prediction is the direct signal, which in simple terms is the value of the loss of the signal sent by the transmitter at the receiver site. Since the coordinates of the latter are unknown, it is necessary to calculate the loss of the transmitted signal at every point in the terrain. Later, the receiver antenna pattern effect will be added to obtain the final value.

The signal losses at every point in the terrain are computed using the *research window* in AREPS, shown in Figure 3.7 and an interpolation routine on Matlab®. The inputs to the most relevant fields on AREPS are described below:

- The terrain file, calculated and stored previously, for 0º bearing will be the input into the *terrain* field.
- The fields corresponding to the transmitter parameters (defined as *EM system parameters* and *Antenna type*) are filled using the data displayed on Table 3.1.
- In the *Atmosphere* field, a file containing meteorological data from a weather station at Albuquerque, New Mexico (AlbuNMjul2001.*env*) will be used.
- The wind option will be set to *Do not use wind*.
- The *Surface type* will be *Rocky Soil* since the topography described by the simulated terrain normally would imply a barren rocky soil.

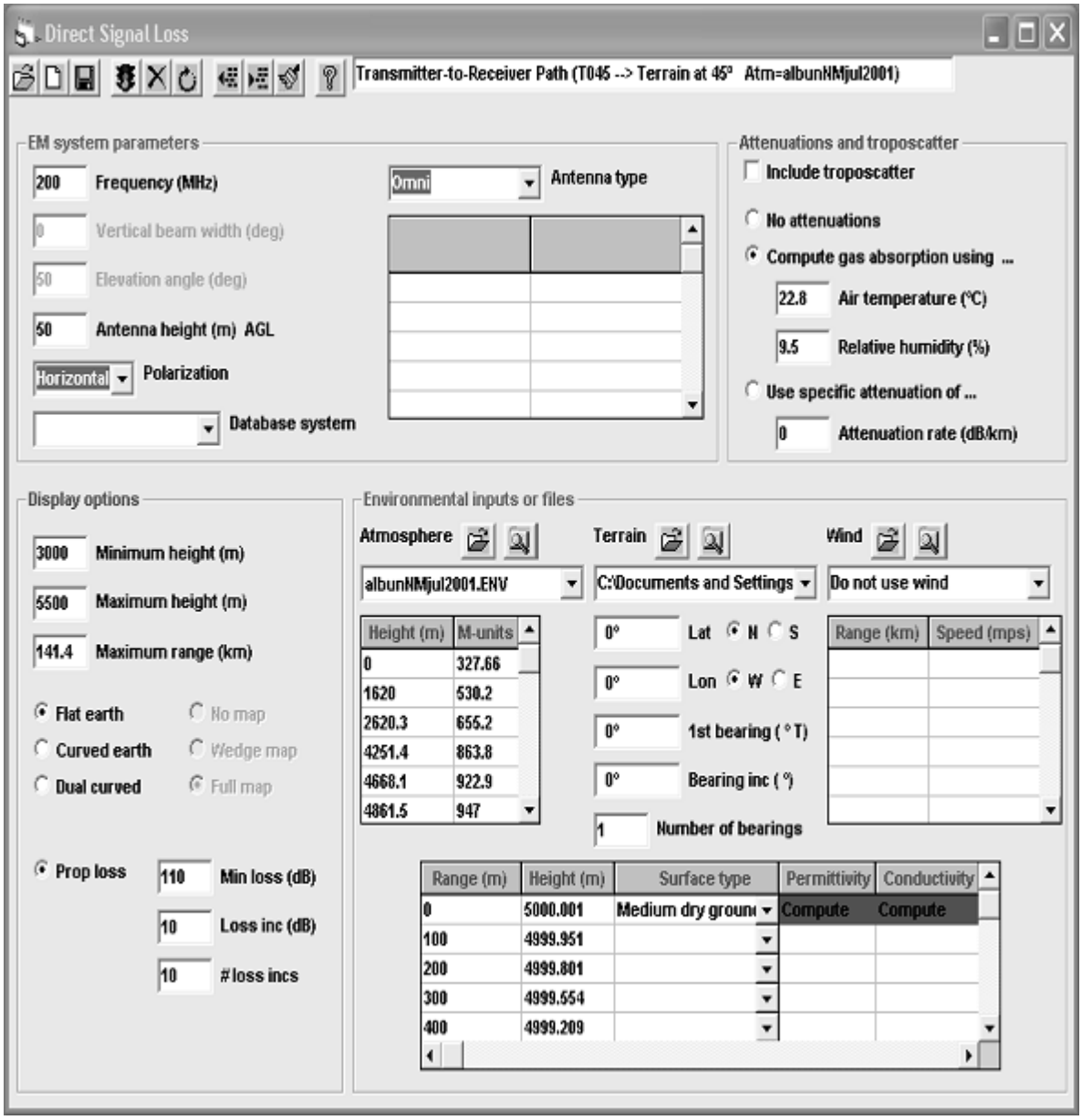

Figure 3.7 AREPS *research* window used to calculate the losses of the signal from the transmitter to every point in the terrain.

Once the information in the fields is completed, as indicated in Figure 3.7, the loss prediction is performed automatically, using the parabolic equation method as detailed in Chapter II. The output is a display showing the terrain profile at the selected bearing, with the height and range scales on the Y-axis and X-axis respectively. In addition, colored regions and its corresponding scale indicate the losses of the transmitted signal. On the right hand side of the window, the values of the geographic parameters, and the loss of the signal at the cursor position are indicated. It is also possible to generate a table of range vs. loss at a specific height. This data chart will be saved as an ASCII file for further process on Matlab®. These two features are presented below in Figure 3.8 and Figure 3.9.

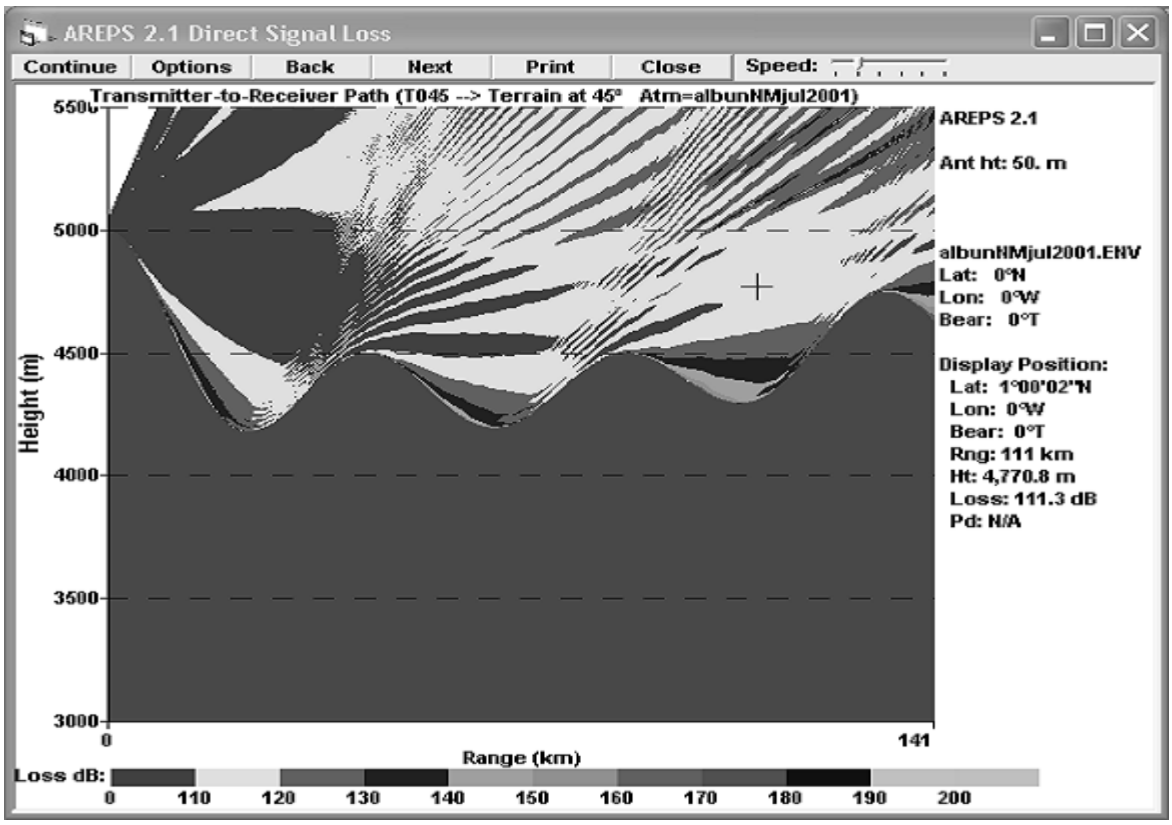

Figure 3.8 AREPS Decision Aid window used to display the terrain profile and the losses of the signal at different ranges and heights.

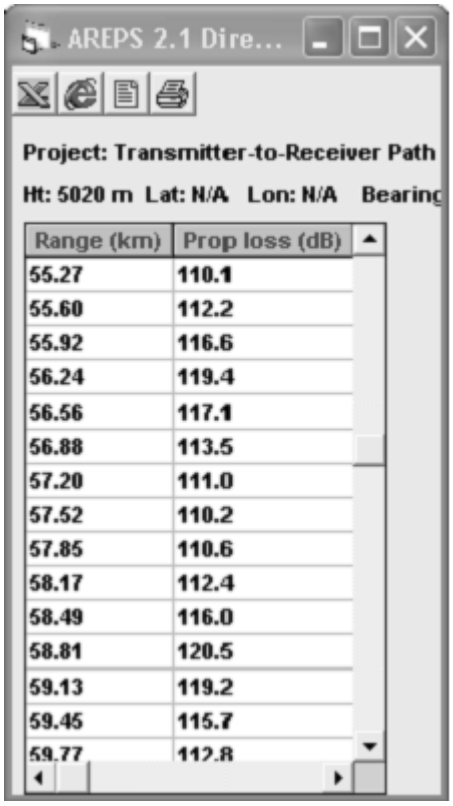

Figure 3.9 AREPS Range vs. Propagation Loss window used to display the losses of the transmitted signal with respect to the range, at a specific height.

To calculate the losses on the other 18 bearings the process is repeated changing the terrain file, and saving the range vs. loss data under a different name to identify the bearing and the height to which it correspond.

The *Maximum range (Km)* field of Figure 3.8, is set to 141.4km ($\sqrt{(100km)^2 + (100km)^2}$). For the terrain files where the maximum range is less than 141.4km, AREPS will extrapolate the loss values at heights above the last elevation specified at the last range. That is, for example, at 15º, the maximum specified range is

110.4km and the height at that range is 4,196.4m. Then it is possible to obtain, not having the need to extrapolate on a separate procedure, a loss vector containing loss values for 141.4 km, for all heights above 4,196.4m.

The receiver can be located anywhere on the terrain, and the receiver antenna can be at any height h_a (within a logical margin). In this case, the antenna height is 20m, as stated on Chapter II. Therefore, it is impractical to generate a chart like the one of Figure 3.9 at every terrain altitude. The proposed solution is to obtain the range versus losses tables at arbitrary heights h where possible, and by extrapolation obtain the loss value at an elevation equal to the terrain height z, plus h_a.

To proceed with the above, the arbitrary set of heights h is 5,050m, 4,800m, 4,600m, and 4,400m. A file with the loss information is created at these elevations where possible. For example at 0º, the terrain profile has only one height, which is 5,000m. Consequently, only one file is generated for that bearing. The criterion is to obtain the data at a certain level when there is at least a portion of air on the terrain profile.

Once the loss files have been prepared for all the bearings and possible heights, they need to be modified in order to process them on Matlab®, because where there is land at the altitude where the losses are being calculated AREPS assigns a value of 0.0. In addition, when there is no terrain defined beyond a certain range, and below the last height defined, AREPS assigns a value of –1.0. Then, when an extrapolation to obtain the loss quantity at a certain height (which will be explained later) is performed, the 0.0 and the –1.0 values will induce erroneous results driving the loss values to an unrealistically low level.

In simple terms a Matlab® code opens all the loss files containing the raw data of range vs. loss. They are saved separately as a matrices **LR** of size nx2, where *n* is the specific number of rows for each particular file corresponding to every particular bearing. The first column is the range data, and the second column is the loss at the corresponding range. The code looks in the second column of **LR** for all values out of the possible range of losses. This can be determined by simple inspection using the *Decision Aid* window of AREPS ([20dB 300dB]). The code eliminates the rows of **LR** where the data is out of scope. Using the original range vector (first column of **LR**) the code performs an interpolation and/or extrapolation dependent upon whether the unwanted values were on the extremes of the vector or in between likely real quantities, to find the possible values at the points specified on the original range vector.

Now, a new range vector **rp** is defined on the interval [0 141,000] at 1000 step intervals. The code finds a new loss vector **lp**, with the processed loss data, containing information at the newly defined range steps. Finally, 19 new matrices $\mathbf{LP}_{142x2}$ are created at each particular bearing, containing the new range vector in the first column and the loss information at each range step in the second column.

Once the loss vectors are modified according to what was stated above, they are converted to Cartesian coordinates to obtain a square matrix the size of the first quadrant, i.e., 101x101. Figure 3.10 gives a pictorial representation of the preceding steps.

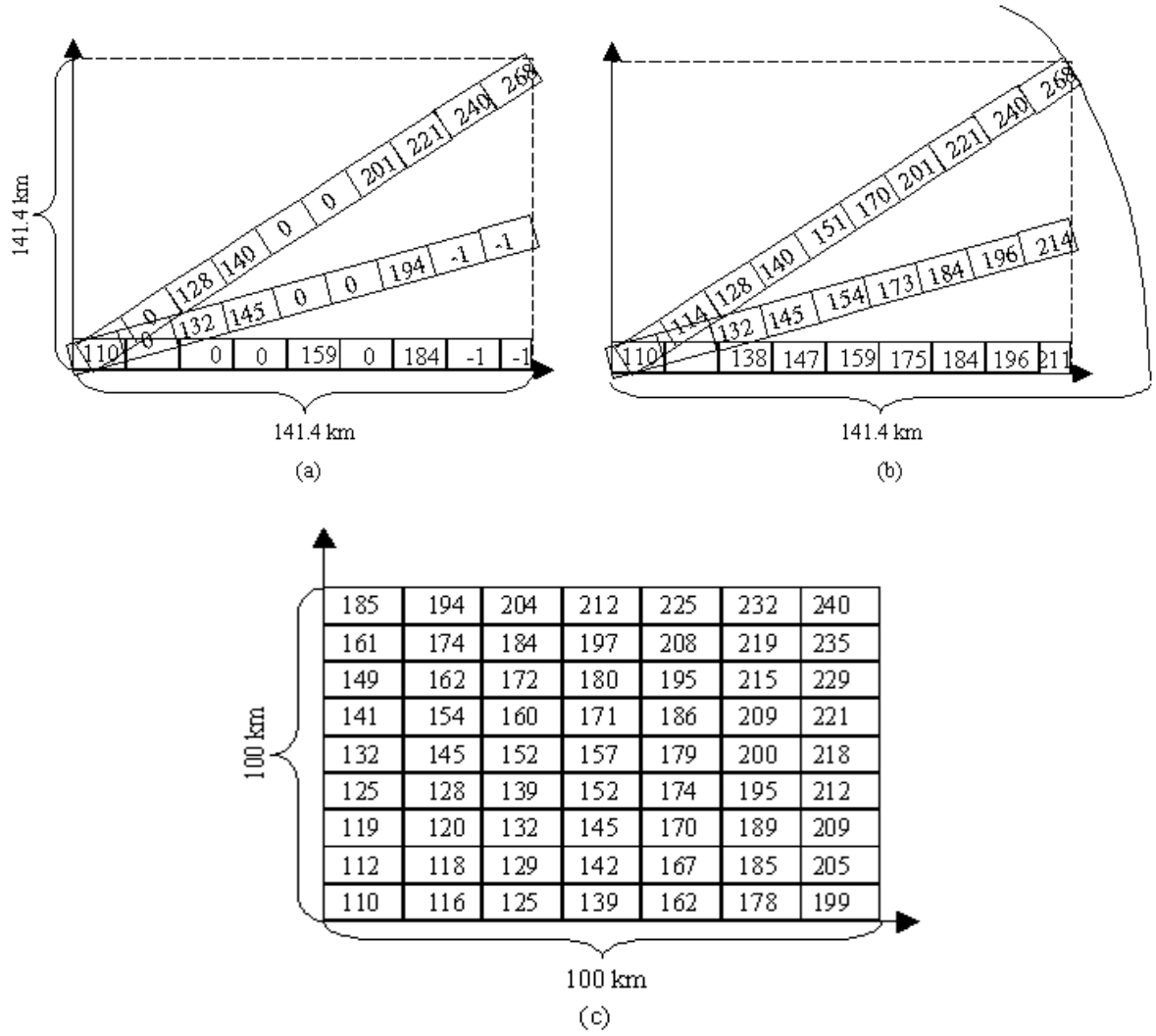

185	194	204	212	225	232	240
161	174	184	197	208	219	235
149	162	172	180	195	215	229
141	154	160	171	186	209	221
132	145	152	157	179	200	218
125	128	139	152	174	195	212
119	120	132	145	170	189	209
112	118	129	142	167	185	205
110	116	125	139	162	178	199

Figure 3.10 The loss vectors layout. a) The loss vectors from the **LR** matrices, containing 0.0 and –1.0 values. b) The loss vectors from **LP** matrices, of the same length and interpolated values. c) The loss vectors corresponding to the same altitude, on Cartesian coordinates.

The conversion of the individual loss vectors in polar coordinates, to a Cartesian coordinate system is performed as follows. Since we need to know the estimated loss at every elevation specified in the matrix **Z** plus some receiver antenna height, we want to obtain a loss matrix **LH** on Cartesian coordinates at the set of heights *h* (5,050m, 4,800m,

4,600m, and 4,400m). The idea is to use the information contained in the **LH** matrices to find the loss at a elevation specified on Z plus the receivers antenna height.

For h = 5,050m, the matrix is fully defined since at that elevation it was possible to perform the loss prediction in all 19 bearings given that all elevations on the terrain are below 5,000m. At h = 4,800m, and subsequent values, it is possible to obtain a more reduced number of loss files. The reason for the latter is that at 4,800m and 0º on the terrain file, there is only ground. However, at 5º there is atmosphere present starting at approximately 57km. Therefore at h = 4,800m there are only 18 loss vectors forming the matrix **LH**. Nevertheless, at h = 4,400m and 5º there is only ground. So for **LH** at this last height there are only 17 loss vectors, i.e., from 10º to 90º every 5º.

To resolve these discrepancies in size of the **LH** matrices, the loss vectors obtained at the same height are ordered on columns. Consequently, the first column corresponds to the losses at the first available bearing, and the last column to the 90º bearing. An extrapolation is performed on every row to obtain the fictitious losses at that height, in case there would be no ground at that level and bearing. Figure 3.11 depicts the above procedure.

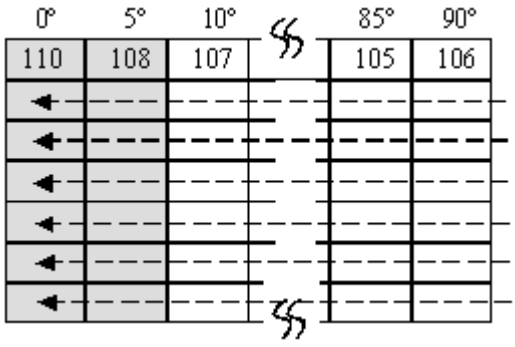

Figure 3.11 Matching the size of the matrix **LH** at 4,800m, 4,600m and 4,400m to the size of the Matrix **LH** at 5,000m obtaining the missing values in the gray boxes by extrapolation of the values in the white boxes.

Once this is done there will be four different **LH** matrices of the same size, one per each value of *h*. The length of the vector rp, used to perform the interpolation to get rid of the 0.0 values and standardize the loss vector lengths, gives the number of rows. That is 142. The number of columns of all **LH** matrices is 19, from the 19 different bearings. Now the four **LH** matrices contain the loss values of the transmitted signals at every cell of the first quadrant for different altitude values. Each value corresponds to a pair of polar coordinates (that was the way they were calculated). These coordinates are stored on two matrices of the same size. One of them, **RHO**, contains the values of the range vector, **rp** ([0 141,000] at 1,000 steps) of length 142, on polar coordinates. The other, **θ**, contains the values of a vector θ_T, defined in the interval [0 90] at steps of 5º, of length 19. These matrices have a similar structure as the matrices **X** and **Y**, shown on Figure 3.3a) and 3.3b). That is, as can be seen below, **RHO** has constant value rows, equal value columns, and a size of 142x19. **θ** has constant value columns and equal value rows, having the same size as **RHO**, as shown in Figure 3.12.

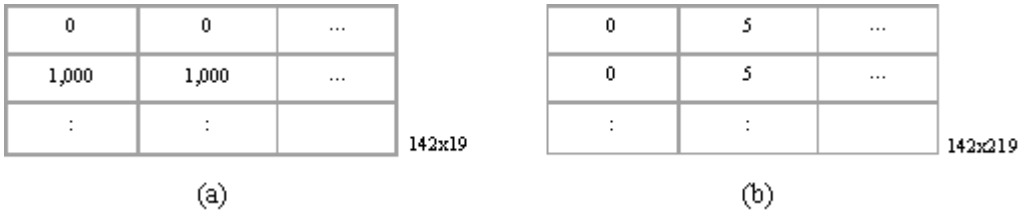

Figure 3.12 (a) The polar range matrix **RHO**. (b) The angle matrix **θ**.

Now the matrices **LH**, **RHO**, and **θ** are ready to be transformed into a Cartesian coordinate grid the same size as the grid used to define the terrain heights on the first quadrant, i.e., 101x101.

First, **RHO** and **θ** are transformed. The result is stored as **XH**, and **YH**. Then, on Matlab®, using **XH**, and **YH**, each of the four **LH** matrices, is processed to find the loss values at the points defined by the coordinates of the first quadrant. Those coordinates are stored on the matrices defined at the beginning of the chapter, **X** and **Y**, on the rows 1 to 101 and columns 101 to 201. The result yields four different matrices named $\mathbf{LDH}_{(101x101)}$ containing the loss values of the transmitted signal to every cell on the first quadrant.

Finally, to obtain the value of the direct signal, at a specific elevation above the ground level, on the first quadrant, a Matlab® code is developed to perform an interpolation or extrapolation according to the scheme presented on Figure 3.13.

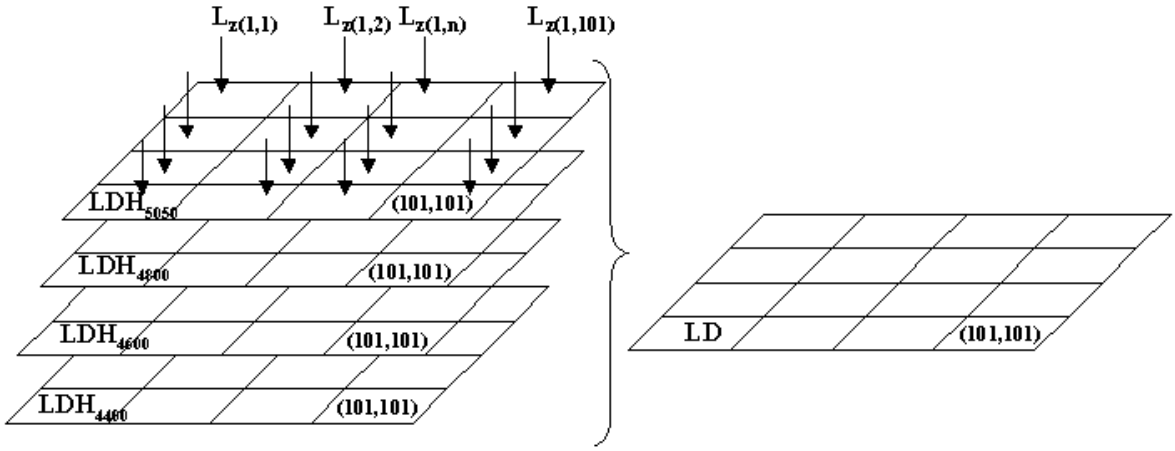

Figure 3.13 The elements of the **LDH** matrices with common indices are grouped into a vector and used to obtain the loss value at the height stored on **Z** with the same indices. The results will be stored in a matrix $\mathbf{LD}_{(101x101)}$ on their corresponding cells.

The scheme presented above, symbolizes the operations performed to obtain the loss of the direct signal, **LD**. The first step is to group the elements of each of the four **LDH** matrices having the same indices. That is, the value contained in $\mathbf{LDH}_{(1,1)}$ at 5,050m, the value contained in $\mathbf{LDH}_{(1,1)}$ at 4,800m, on so on. The four values are stored in a vector **ld**.

The second step is to create a vector **h** = [5,050 4,800 4,600 4,400]. Then, the height value contained on $\mathbf{Z}_{(1,1)}$ plus the receiver antenna height h_a is compared with the values of **h**. If $\mathbf{Z}_{(1,1)}$ is in between 5,000 and 4,400 an interpolation routine is used, to find the value of **ld** at that elevation. Otherwise, an extrapolation method is applied. The result is stored in a matrix **LD** at (1,1). The same procedure is applied to every single element of **Z**. The result yields a matrix $\mathbf{LD}_{(101x101)}$ containing the loss of the direct signal, for the first quadrant.

The loss for the whole terrain area is obtain, as shown in Figure 3.14, by flipping $\mathbf{LD}_{(1:100,1:101)}$[4] upside down. The two matrices are concatenated, forming a new $\mathbf{LD}_{(201x101)}$ matrix. Finally, $\mathbf{LD}_{(1:201,2:101)}$ is flipped left to right and concatenated again. This yields the final matrix $\mathbf{LD}_{(201x201)}$, as shown in Figure 3.14

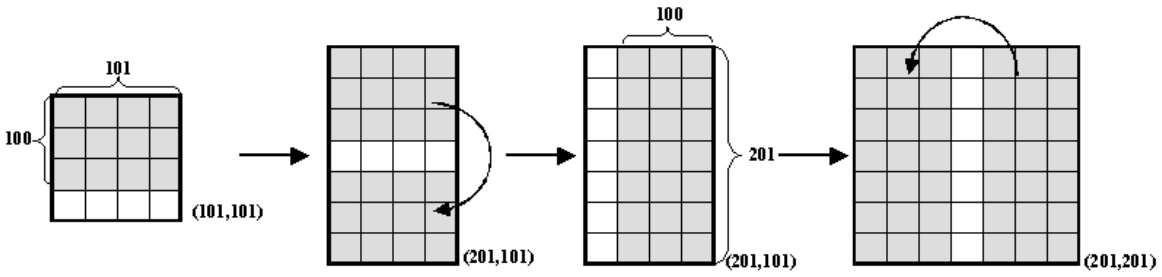

Figure 3.14 Obtaining the loss matrix of the direct signal, for the whole terrain grid, from the original $\mathbf{LD}_{(101x101)}$ matrix, corresponding only to the first quadrant.

3.3.2 Adding the Receiver Antenna Pattern Effects. The values obtained by the above method are just partial values. These quantities are the losses of the direct signal arriving at the possible receiver site. The logical procedure would be to subtract to the transmitter power P_T the calculated loss, but this result will not take in to account the effects of the receiver antenna. To know the impact of these effects is very important, since the direct

[4] The notation $\mathbf{M}_{(1:m,1:n)}$ means rows 1 to m, and the columns 1 to n of matrix **M**.

signal will compete with the signal coming from the object. So, once the losses of the direct signal are obtained the effects of the receiver antenna pattern must be added.

In simple terms, the next step is to find the angle of the antenna pattern *az* with respect to the maximum direction of gain, based on the values of the angle of arrival of the direct signal at the receiver site, and the pointing angle of the antenna when looking to the AOI.

The location of the receiver is yet unknown. However, the AOI has been defined and the assumption that the object is located on the main lobe of the antenna was stated. Since, up to now, the receiver can be located on every coordinate of the terrain, the antenna pointing angle is calculated as if the antenna would be looking from every possible location to the coordinates (17km, 100km). That is considering only the first and fourth quadrant. The pointing angles for the whole terrain are obtained by flipping the resultant matrix left-to-right and concatenating both matrices.

To execute these calculations a Matlab® code is written using the following considerations. The direction of the direct signal can be expressed using the θ_T angle. The pointing angle of the receiver antenna can be expressed by θ_R.

These angles are calculated according to the relations:

$$\theta_T = \tan^{-1} \frac{(X - 0)}{(Y - 0)} \tag{3.3a}$$

and

$$\theta_R = \tan^{-1} \frac{(17 - X)}{(100 - Y)}, \tag{3.3b}$$

where X and Y represent the coordinates of the terrain, the 0 values on (3.3a) are the coordinates of the transmitter, and the 17 and 100 values on (3.3b) represent the receiver coordinates. Figure 3.15 exemplifies the geometry being used.

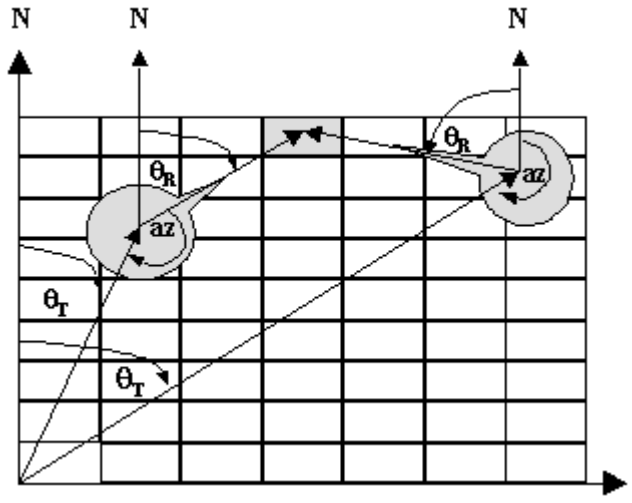

Figure 3.15 Geometry to calculate the angle of the antenna pattern (on gray), with respect to the maximum direction of gain, *az*, by calculating the angle of arrival of the direct signal to the antenna pattern and the antenna pointing angle of the direct signal, both with respect to the North reference axis.

To determine the values of *az* the following relationships are established based on the location of the receiver with respect to the AOI and the transmitter:

$$\text{az} = -\left(180 - \theta_T - \left|\theta_R\right|\right), \tag{3.4a}$$

when the coordinates are at the right or exactly below with respect to the AOI, then

$$\text{az} = 180 - \theta_R + \theta_T , \tag{3.4b}$$

when the coordinates are at the left of the AOI and above the transmitter, and

$$\text{az} = -180 - \theta_R + \theta_T , \tag{3.4c}$$

when the coordinates are left of the AOI, and at the Y = 0 level or below the transmitter.

The results obtained are stored in matrix $\mathbf{AZ}_{(201\text{x}101)}$. Then, a second code extracts from a matrix $\mathbf{AP}_{(360\text{x}2)}$ the antenna pattern values corresponding to the azimuth (whole values on the interval [-180º 179º]), on the first column, and the gain (in dB), from the second column. With these quantities, the code finds, by interpolation, the exact value of the gain at the azimuth determined by *az*. The outcomes, representing the receiver antenna gain are stored in a matrix $\mathbf{AG}_{(201\text{x}101)}$. The values for the whole terrain are obtained performing the flipping and concatenation explained previously for the matrix **LD**.

Now, finally the data needed to calculate the received power of the direct signal, at the possible receiver locations, P_r, is available. Then the direct signal power (in dB) at every coordinate of the terrain is:

$$P_r = P_T + G_t - LD + AG . \tag{3.5}$$

Equation (3.5) represents the power of the transmitted signal at the receiver. The receiver antenna is pointing at the AOI. The transmitted power is increased by the

transmitter antenna gain, then attenuated by the losses caused by the terrain and the atmospheric conditions at the moment of propagation, and finally, is affected by the receiver antenna. This last variation increases or decreases the signal power depending on the location of the receiver as explained earlier. The result of equation (3.5) is stored in a matrix $\mathbf{DS}_{(201x201)}$.

3.4 The Transmitter-To-Object Path

The transmitter-to-object path is a straightforward process. The location of the object is known from the definition of AOI. It is required to determine the angle of the AOI from the positive Y-axis, θ_T, and to calculate the terrain file at that bearing. Then that file is used as input on AREPS. The loss value of the transmitted signal at the object, L_{tgt}, will correspond to that at the maximum range and at the corresponding flight level. The strength of the signal arriving at the object will be the transmitted power P_T plus the gain of the transmitter antenna G_t minus the loss at that point L_{tgt}.

As well as in the Transmitter-to-Receiver path, the following calculations are performed only in the first quadrant. The case for the second quadrant is similar, being the angle with respect to the North reference of opposite sign.

The specific location of the AOI is at the deepest valley ($\mathbf{X}_{(1:201,118)}$ = 17km) on the northern limit of the terrain ($\mathbf{Y}_{(1:1:201)}$ = 100km), and 100m above the ground ($\mathbf{Z}_{(1,118)}$+100=4,279.8m). Therefore, the distance from the transmitter to the object on the horizontal plane is approximately 101,435km ($\sqrt{(17km)^2 + (100km)^2}$).

To determine the angle θ_T, with respect to the North, the *arctan* function is used according to Figure 3.16.

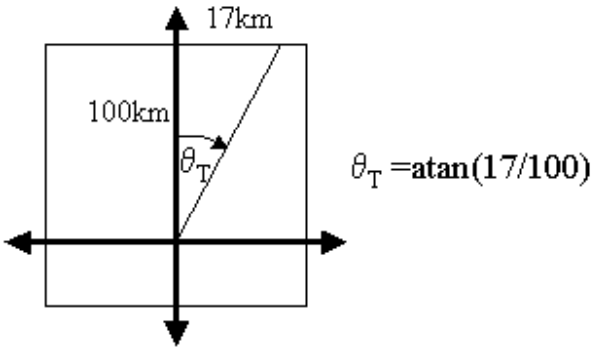

Figure 3.16 The geometry for the Transmitter-to-Object path.

Solving for θ_T, the result yields 9.7º. The new terrain file is determined by using the same code previously utilized. This file is then processed by AREPS. To determine the loss value at the object, on the *Decision Aid* window, the cursor is located at the range and height of the AOI. The loss value appears on the right hand side of the window. A general example of this can be seen in Figure 3.8. In the case that the exact range and height do not show, a second approach is used.

As previously stated, it is possible to generate a chart of loss versus range similar to the one in Figure 3.9 at 4,279.8m, or a table of loss versus height at 101,435m of distance from the origin. Then by interpolation of the data on the chart the estimated loss value is found at the desired range and elevation.

Once the loss value of the direct signal at the object is determined, it is subtracted from the sum of the transmitted power plus the transmitter antenna gain. This new result represents the transmitted signal at the object and is stored as a constant, P_{tgt}. By including

the radar-cross-section, the value of the scattered signal from the object is obtained as stated by:

$$P_{tgt} = P_T + G_t - L_{tgt} + \sigma_B . \tag{3.6}$$

Equation (3.6) represents the value of the first path of the indirect signal. Similar to equation (3.5), the transmitted signal power is increased by the transmitter antenna, then attenuated by the effects of propagation, and finally affected by the radar-cross-section of the object.

3.5 The Object-To-Receiver Path

This calculation is similar to the two previous cases and uses the same concepts. The main differences are that the terrain files must be redefined, and that the effects of the receiver antenna pattern are included on the loss predictions.

Since we are looking for the receiver location we cannot predict the look angle, or where and how the receiver antenna will affect the scattered signal from the object. We can only make the assumption of the location of the object based on the need to optimize the PCL system to perform a specific task. Given this, it is possible to use the antenna reciprocity theorem. In simple terms, the object is considered as a transmitter. This is true in the sense that the object is the source of the indirect signal for the receiver. Now we can assign the receiver antenna pattern to the object location. Again, given that the system will be designed to provide early warning against a object coming from a specific sector where other sensors have a lack of coverage, wherever the receiver location may be, the direction of maximum gain will always be toward the AOI.

As in the Transmitter-to-Receiver path case, the first step here is to define the terrain files. Because AREPS imposes a restriction that the transmitter must be located at the origin of the terrain profile, i.e., at 0 m range, the terrain files must be redefined. One option is to place the coordinate system at the AOI location. That is, at (x,y) = (17km, 100km)[5]. Instead of evaluating the generating function on **y** = [-100 100], this is done by evaluating it on **y** = [-200 0]. Once the equation is evaluated, it is necessary to relocate the **X** matrix 17 units to the left. That is, **X** - 17. At this point, the **Z** matrix remains constant, and the X and Y coordinates were shifted by 17 and 100 units to the left and down, respectively; i.e., the origin of the coordinate system has been relocated and placed at the AOI. This reassignment of coordinates leaves a terrain defined only on a new third and fourth quadrant of 100km by 200km each, as depicted below in Figure 3.17.

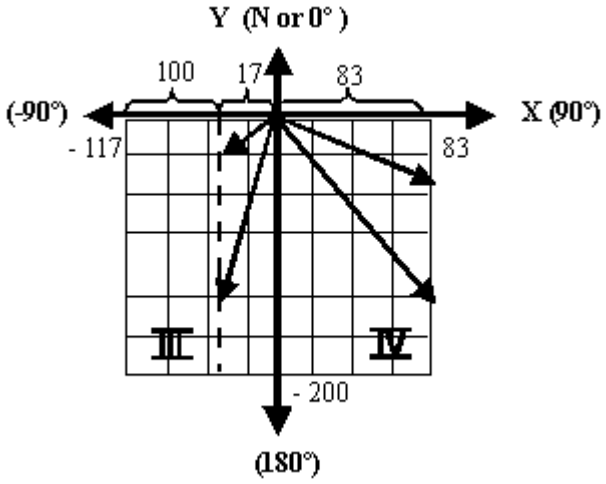

Figure 3.17 The new coordinate system, centered at the AOI, keeping the same terrain grid dimensions and the same values on the elevation matrix **Z**. Also shown on the scheme is a representation of the vectors on the directions the new terrain files will be defined.

[5] In this section, only the case of the AOI on the first quadrant will be treated. The same procedure applies to the AOI located at (-17km, 100km). The result on that case will be similar as of the first quadrant AOI, but with the loss matrix flipped left-to-right.

The terrain files are created using the same procedure detailed at the beginning of this chapter. Due to the location of the object (deep within the valley on the original first and fourth quadrants), and the weakness of the echoes, it is reasonable to assume that the receiver cannot be placed anywhere in the initial second or third quadrant. Therefore, the terrain files are generated from a grid, which specifies only the terrain on the original first and fourth quadrant. The angles of the terrain represent the values of θ_R, as can be seen in Figure 3.18. They go from 90º to 180º, corresponding to the new third quadrant, and from –90º to –175º, corresponding to the new third quadrant. The total number of files will be 37.

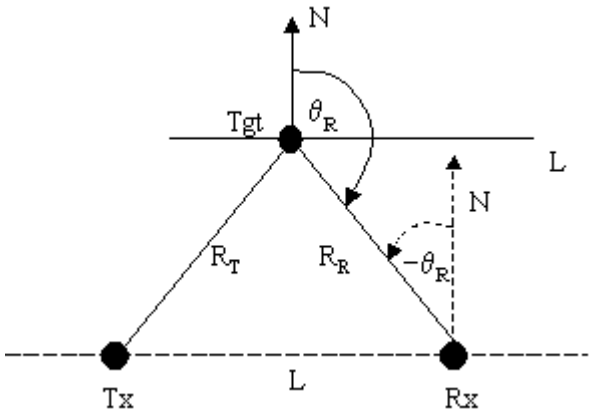

Figure 3.18 The angle θ_R, assigned to the terrain files, according to the sign convention of the North-reference coordinate system. Here the base line and the North axis are placed at the object location.

As occurred in the previous cases the terrain files need to be reprocessed using a polynomial regression to clear out the noise originated when generating the files.

Once the terrain is ready and the power of the signal at the object has been calculated, it is necessary to focus attention on the effects of the receiver antenna pattern.

AREPS includes on the *Research window* (Figure 3.7) the option to define the antenna type to be used at the source. Choosing from the antenna drop menu the option *user defined* does this selection. Here the antenna pattern on the horizontal plane can be expressed on dBi, or as a normalized value. The latter will be used. Now it is possible to import a file containing the horizontal normalize antenna pattern to be used, stored as a matrix $\mathbf{APN}_{(nx2)}$. The first column contains the bearing values expressed in degrees, and the second column the normalized gains values. One of the requirements is that the maximum normalized gain value, that is 1, needs to be characterized at 0º.

When the *user defined* selection is chosen the *Elevation angle (deg)* option becomes active. The angle is referred to as the angle above the local horizontal of the antenna pattern.

The matrix **APN** will remain unchanged at every bearing, due to the fact that wherever the receiver is located its antenna main beam ideally will be pointing at the object. In other words, keeping in mind that the receiver antenna has been located at the object location, the main beam will always be pointing toward where the loss prediction is being calculated, otherwise, the loss calculations would be performed from every terrain cell, pointing the antenna at the expected object location.

The values of the antenna elevation angle will vary depending where the receiver is with respect to the object. To be exact, for the terrain located inside of the mountains forming the valley, if the receiver is above the object, the true elevation angle of the antenna at the receiver site will be negative. Having the antenna located on the object, the

angle will have the same value, but with a positive sign. If the receiver is at a higher elevation than in the previous case, the angle will still be negative since the receiver will be looking downward, but the value will be higher. If the receiver happens to be lower than the object, the value to be used on AREPS will be negative.

There are two important points worth mentioning. The first is that AREPS, when using the option *user defined antenna* the *beamwidth* field is not active. The second point is that in general, for the terrains and environments used for testing during this research, the difference in dB between two AREPS runs, one using 0º elevation angle and the other with 10º, was around 1dB or less. Therefore, even though the methodology to calculate the elevation angle is presented next, it is not strictly necessary to use the resulting values on the propagation loss calculations. The reason is that the highest possible elevation angle is 2.5º, at –90º. That is when the receiver antenna is located at the closest highest elevation with respect to the object, i.e., at 17km of range, 5,000m of height and –90º of bearing.

To calculate the loss of the signal, the same approach as in the direct signal case will be used. That is, the loss of the scattered signal will be calculated at different altitudes. For that reason, as in the Transmitter-to-Receiver path case, a set of elevations h will be defined. Then, at every bearing, the loss prediction software will be run, using the same antenna pattern, at the corresponding elevation angles, as if the receiver antenna would be located at that elevation, looking toward the AOI.

In synthesis, the idea is to select a bearing. Then, select the antenna pattern and specify an elevation angle previously calculated for a particular height h_1. The next step is to generate a table containing the loss values versus range at that particular altitude h_1. Among the results, the loss corresponding to the range r_1, will be equivalent to the actual

value of the loss of the indirect signal coming from the object, when the receiver antenna is located at the coordinates (x, y, z) defined by r_1 and θ_R, and the antenna is pointed to the object. After that, to continue with the calculations, a change on the elevation angle is performed according to the second height h_2 and so on. When the signal loss is calculated at all heights the next terrain file is used and the same procedure applied. Figure 3.19 helps to visualize these ideas.

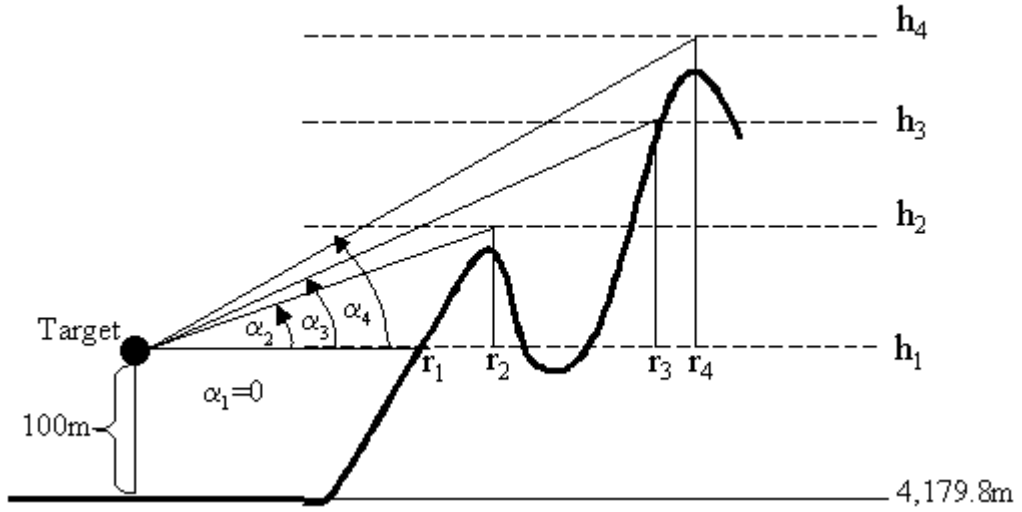

Figure 3.19 Calculating the Object-to-Receiver path at a particular bearing. By predefining a set of heights h_1, h_2, h_3, and h_4 is possible to calculate the ranges r_1, r_2, r_3, and r_4 and therefore the elevation angles α_1, α_2, α_3, and α_4

As implied before, the angle values must be obtained before the loss calculations. To do that for a particular bearing using Matlab®, the corresponding terrain file is opened and, as before, the range information is stored as a vector **r**, and the height data as vector **h**.

The specific range value r_n at a height h_n will be found by interpolating the vector **r** at the height h_n.

The set of elevations h will be defined based on the existing terrain elevation values. For example, on the fourth quadrant of the new terrain there are three heights easy to identify for posterior verification of the results. One is the object flight level, which is approximately 4,280m. The second elevation is the top of the mountain right next to the object at 4,500m plus the antenna height h_a = 20m, i.e., 4520. The last one corresponds to the highest elevation on that quadrant, which is approximately 4750m plus h_a, or 4770m. On the fourth quadrant, besides the flight level the other relevant feature of the terrain is the highest elevation of the whole terrain plus the receiver antenna. That is 5,020m. In summary, the set of height values to be used on the calculation of the losses of the indirect signal are h_1 = 4,280m; h_2 = 4,520m; h_3 = 4,770m; and h_4 = 5,020m. However to calculate the values of the elevation angles, the heights to be used are those that are above the flight level of the object. Therefore, they are $h\alpha_1 = 0$; $h\alpha_2 = h_2 - h_1$ = 240m; $h\alpha_3 = h_3 - h_1$ = 490m; and $h\alpha_4 = h_4 - h_1$ = 740m.

Up to this point, we have the value r_n obtained by the aforementioned interpolation process using h_n, and the height above the flight level $h\alpha_n$. Now by simple use of the relation α_n = arctan ($h\alpha_n$ / r_n) it is possible to calculate and store those values as the elevation angles, which are to be used for the Object-to-Receiver path loss predictions at every bearing.

Now, all the inputs needed by AREPS to perform the loss prediction at every bearing are ready. The procedure is the same as indicated for the direct signal case. That includes the generation of the loss matrices with the raw data, **LR**, the processed loss matrices **LP**, and the matrices **LH**, containing the losses of the indirect signal at every height h in polar

coordinates, as well as in Cartesian coordinates after being transformed from the previous coordinate system.

For this last particular matrices **LH**, they will all be of the same size. Due to the fact that when calculating the direct signal it was not possible to calculate the losses at all heights because there was only terrain at certain bearings, the **LH** matrices did not have the same dimensions. Now, since the object is in the air, it is possible to generate a loss vector at every bearing for the set of heights *h*.

The generation of the matrix containing the loss values of the indirect signal **LIH** will be of size (201x101) since each value, as before, will represent the loss at every particular terrain cell 20m above the ground level (because of the antenna elevation). Then, the same procedure used to obtain **LD** applies to obtain a single matrix $\mathbf{LI}_{(201x101)}$ with the interpolated (or extrapolated where applies) loss values at the terrain height plus the antenna elevation. Once again, from that matrix the loss of the indirect signal matrix covering the whole terrain is formed.

Finally, all the necessary data, to calculate the received power of the indirect signal can be obtained. As presented on equations (3.5) and (3.6) the value of the power of the indirect signal can be expressed as:

$$P_r = P_{tgt} - LI + G_r \tag{3.7}$$

Here, the received power is the result of the power coming from the object, calculated on equation (3.6) minus the propagation loss, plus the maximum gain of the receiver antenna. The maximum gain value is used since the assumption that the receiver antenna

will be pointing at the AOI was made. The result of equation (3.6) will be stored on a matrix $\mathbf{IS}_{(201x201)}$.

3.6 The Location of the Receiver

The problem of defining the receiver location on a PCL system consists basically in determining the regions where the power of the direct and indirect signal at the receiver reach an acceptable level to process them in order to perform detection of objects on a specific AOI.

In the preceding sections two matrices were calculated. The first one was the matrix $\mathbf{DS}_{(201x201)}$, containing the power of the direct signal at every point of the terrain. The second matrix was $\mathbf{IS}_{(201x201)}$ with the indirect signal power.

Two facts need to be taken into account. The first is that the threshold level of the receiver obtained using equation (2.16) was set to be –180dBW. This number limits the possible location of the receiver to only the terrain coordinates represented by the indices of the cells on the matrix **IS** where the value is equal or greater than –180. That is,

$$P_{tgt} - LI + G_t = IS \geq -180 . \tag{3.8}$$

The second fact is that the direct signal cannot interfere with the signal coming from the object. It is reasonable to expect that the direct signal in most of the terrain will be stronger than the indirect one. That situation will probably generate an output on the processor of the system, of an object located at the transmitter coordinates, and with 0

Doppler shift. Filtering the direct signal, as was shown on Figure 2.8, solves this problem. The value of the filter to be used will be set, arbitrarily, to 80 dB considering the empirical values of the filters used on [12] and [13]. In other words, the direct signal has to have less power than the signal the system aims to detect. Then, the direct signal must comply with the inequality:

$$(P_T + G_t - LD + AG) - 80 = DS - 80 < IS, \tag{3.9}$$

where, as a reminder, P_T is the transmitted power, G_t is the transmitter antenna gain, **LD** is the loss of the direct signal matrix, **AG** represents the receiver antenna gain, and **DS** is the direct signal power matrix.

Therefore, the solution space will be defined by the intersection of the set of those coordinates where the indirect signal power is greater or equal to –180dBW, and the set of coordinates where the direct signal power after being filtered is equal or less than the indirect signal power. That is, the final result will be obtained by finding the coordinates within that region where the signal coming from the object is equal or greater than the signal coming from the transmitter, and above –180dBW.

Thinking in terms of the ambiguity function of a radar, if the transmitted signal is a long cosine modulated pulse at a constant frequency: for one pulse the direct signal will generate a triangular ridge along the 0 Doppler axis (the autocorrelation of a square pulse is a triangle) of minimum thickness (the Fourier transform of a Cosine is a delta function). Then, the indirect signal can be distinguished from the direct one if it is shifted on the Doppler axis, and the power is equal or greater.

3.7 Summary

This chapter established the methodology to determine the possible location of the receiver on a PCL system based on a given scenario which includes the terrain, atmospheric parameters, an area of interest and the needed signal levels.

First, the general scenario was described, including the terrain generating functions, the matrix notation to be used, and the way the data needs to be formatted for further process on AREPS. Then, a description of the meteorological data and the way it can be converted into an input for the propagation software tool was explained, followed by the method to calculate the signal loss and the signal power on the transmitter-to-receiver path. After that, the methodology for the calculations of the transmitter-to-object path and for the object-to-receiver path was presented. Finally, the criteria to determine the receiver location based on the power levels at the receiver of the direct and indirect signal is established.

IV. Results and Analysis

4.1 Introduction

This chapter presents the results obtained when using the methodology discussed previously. It is accompanied with a brief summary reviewing the process involved in the generation of the results.

Calculations of the signal loss for the three signal paths are presented, followed by the values obtained corresponding to the direct and indirect signal power. To finish, the possible receiver locations are shown according to the criteria established in the preceding chapters.

4.2 General scenario

There are three main aspects defined within the definition of the general scenario. The terrain, the location and operational parameters of the transmitter, and the region where the system is intended to provide detection.

Equations (3.1a) through (3.1g) were used to generate the terrain surface. The coordinate system, along with the height matrix was stored on a file, to serve as the input for all the following Matlab® codes used in the needed computations. To perform loss calculations on the direct signal path, and the effects of the receiver antenna, a separate file was created to store the data corresponding only to the first quadrant.

In addition, the transmitter location and the area of interest where the system should perform the detection of incoming objects were established. These features are depicted in Figure 4.1.

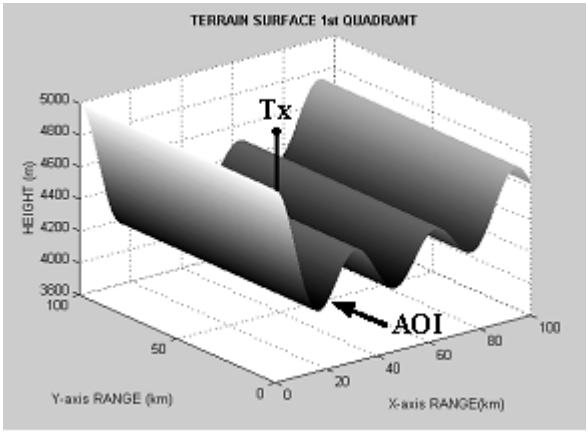

Figure 4.1 Representation of the first quadrant of the terrain surface, used to calculate the direct signal loss, showing the transmitter location. The arrow indicates the valley where the AOI is located, at the coordinate (17km, 100km, 4,279.8m).

4.3 Meteorological Summary

The meteorological data, employed in all loss predictions, corresponds to a weather station located in Albuquerque, New Mexico, on July 06 2001, at 12:00 GMT.

From the information in text format, it is possible observe that the atmospheric pressure and the humidity (water vapor) decrease with the height above the terrain, and to detect a slower increase rate of the temperature. These conditions generate a standard atmospheric condition.

From the summary of propagating conditions generated by AREPS shown in Figure 4.2, it can be seen that the gradients of the plots *N*-units vs. height and *M*-units vs. height

are constant and with a negative and a positive rate, respectively. This implies there are no abnormal conditions present such as inversion layers, evaporation ducts, subrefraction regions, etc.

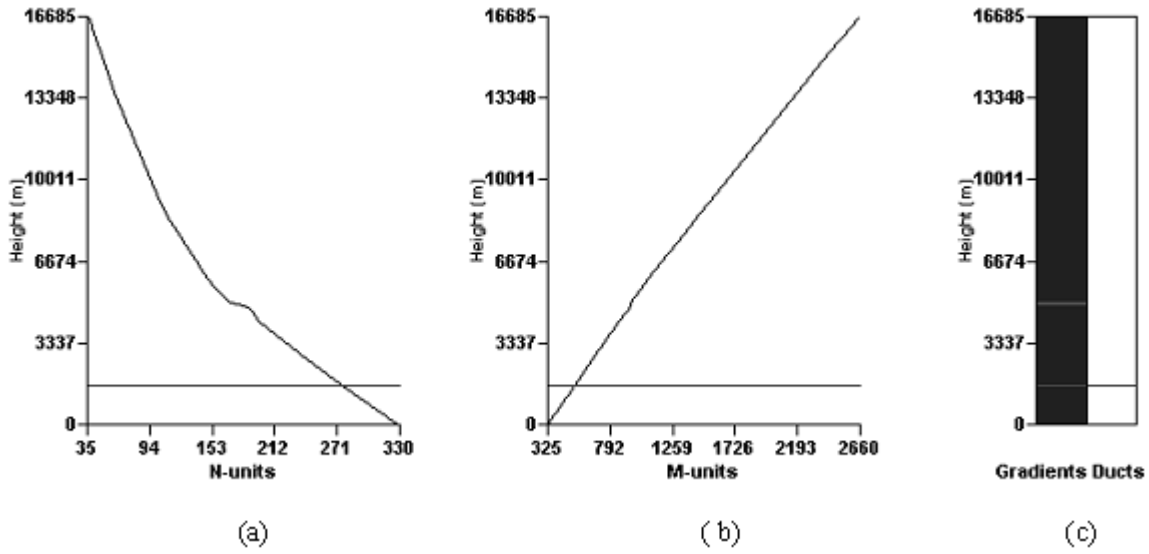

Figure 4.2 Summary of the propagating conditions. (a) *N*-units vs. height. (b) *M*-units vs. height. (c) Stratification layers vs. height.

In summary, the facts presented lead to the conclusion that, at the altitudes where the signal would propagate, the atmospheric parameters present a standard atmospheric propagation condition. This suggests the propagating waves will bend downward as they advance in time and space.

4.4 The Direct Signal without the Effects of the Receiver Antenna Pattern.

According to the methodology presented in the previous chapter, the losses along the direct path are calculated first. The process starts by computing the signal loss at different

predefined altitudes, using: AREPS, terrain files previously prepared, and the meteorological data. These altitudes, representing flight levels, are 5,050m, 4,800m, 4,600m, and 4,400m. The results obtained by AREPS at every bearing, in vector format, were processed on Matlab®. The results for this path are presented in Figure 4.3.

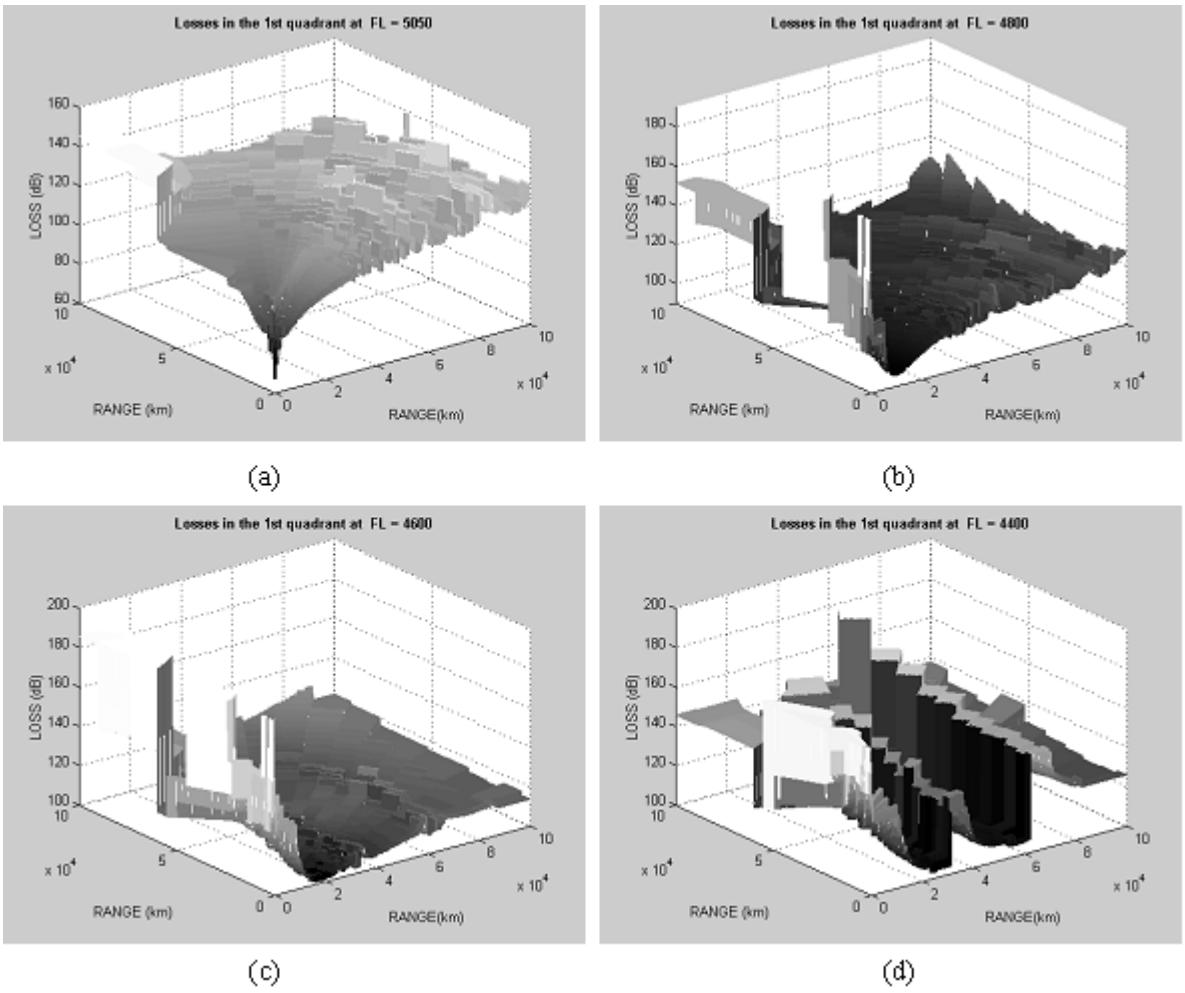

Figure 4.3 Signal propagation losses, in dB, from the transmitter, within the first quadrant at:
(a) 5,050m. (b) 4,800m. (c) 4,600m. (d) 4,400m.

The plots represent the direct signal loss at every coordinate in the first quadrant. As expected, the minimum loss value occurs at the origin of the quadrant (the transmitter site)

and increases toward the boundaries of the terrain region. In Figure 4.3(a) displaying the signal loss at 5,050m, the attenuation increases rapidly near the (0,0) point, and the rate of increment diminishes in a logarithmic type fashion. The reason is that at 5,050m the terrain has a minimum effect on the propagating waves, being the atmosphere the main reason for attenuation. The effects of the terrain on the remaining plots are notorious, and are more explicit because the flight level is closer to the ground; especially the one corresponding to the loss at 4,400m. The clearest effect on these plots is one introduced by the central elevation of the terrain, located along the Y-axis. Here the loss of the signal reaches its maximum. Furthermore, there are two regions that run parallel to the Y-axis where the loss increases noticeably. The closest one to the Y-axis is located approximately between X = 30km and X = 40km which corresponds to the eastern side of the peak located at X = 31km. A similar increase on the loss value is observed roughly between X = 60km and X = 70km. Those coordinates correspond to the eastern side of the second elevation from the origin, at X = 63km.

This brief description of the previous partial results confirms that the procedure to obtain the signal loss is correct. The abrupt changes on the loss numbers are the result of the approximation method used; however, the values are within the expected margin. These statements were verified by using the *Decision Aid Window* on AREPS, locating specific points over the terrain at specific bearings and comparing the values presented on the display with those on the plots in Figure 4.3.

The second stage of the process to obtain the direct signal loss at every coordinate on the terrain was to calculate the loss at 20m above the ground level (the altitude designated for the receiver antenna) using the previous results.

The outcome can be observed in the plots of Figure 4.4.

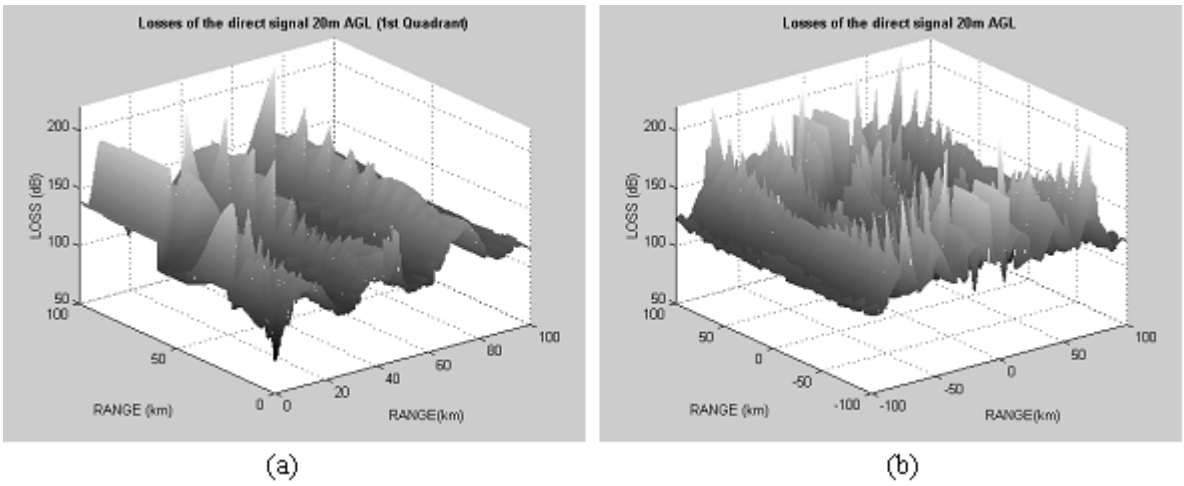

Figure 4.4 Signal propagation loss at 20m above the ground level, on:
(a) First quadrant. (b) Whole terrain.

The result is similar to the previous analysis; a low loss value toward the center of the terrain, the minimum 78.43dB at (0, 0, 5,020m), and greater losses behind the main elevations and toward the limits of the terrain. These results do not represent the final value of the signal at the possible receiver site. The effects of the receiver antenna pattern must be taken into account.

4.5 Adding the Receiver Antenna Pattern Effects.

The reflected signal coming from the object must *compete* with the direct signal approaching directly from the transmitter. If the latter is too strong the receiver will not be able to detect and process the first one. This situation is partially solved by the receiver antenna pattern. If the direct signal reaches the receiver from the back of the antenna, or

wherever there is a null, the signal will hopefully be attenuated enough to allow the receiver to process the signal coming from the object. Since the possible locations of the receiver are yet unknown, in order to calculate the direct signal power at the receiver site, the angle formed between the main beam of the antenna and the North axis is calculated at every coordinate of the terrain. Then, the angle of the receiver antenna pattern at which the transmitted signal reaches the receiver site is computed.

The resulting values, representing the gain of the direct signal at the receiver site, are plotted in Figure 4.5.

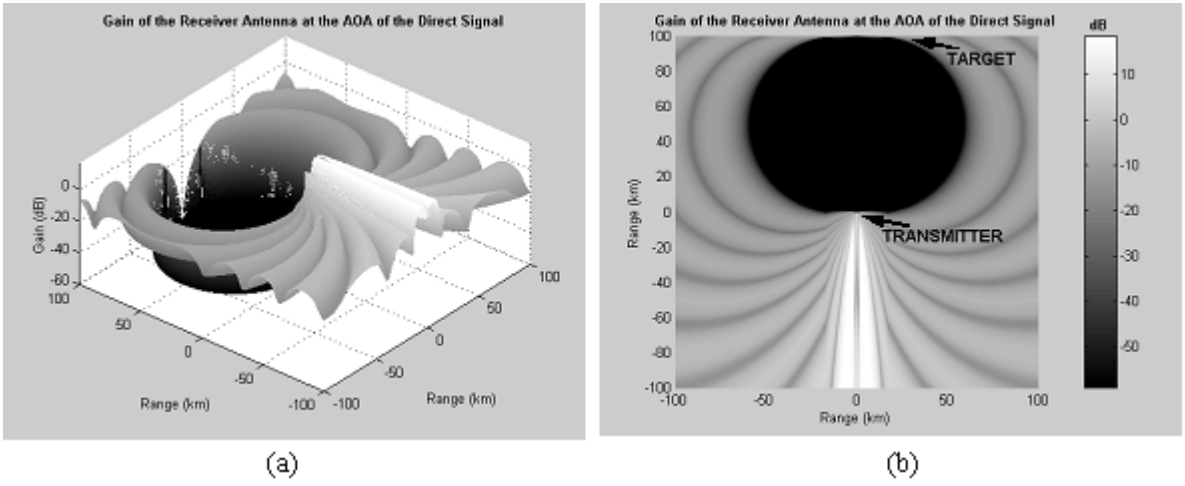

Figure 4.5 Receiver antenna gain at the angle of arrival of the direct signal, when the receiver antenna is aimed at the AOI. (a) Elevated view. (b) Top view.

Figure 4.5 represents the gain level of the receiver antenna when including the whole terrain. As explained in Chapter III, there are two AOI. Due to the symmetry of the terrain with respect to both axes, one is located at the right of the X-axis exactly at (17km, 100km, 4,279.8). Because of the terrain symmetry, the other AOI is located exactly at (-17km,

100km, 4,279.8m). Figure 4.5(a) pictures the differences on the gain values as the location over the terrain changes. The arrows on Figure 4.5(b) indicate the position of the transmitter, and the expected location of the object, on the AOI at the right of the X-axis. In this figure it is also possible to see the clear boundary between the region where the transmitted signals hit the receiver antenna on the back null, and where the signal access the receiver through the main or side lobes.

It is clear that if the receiver is located between the transmitter and the AOI, the main beam will be in front of the receiver looking away from the transmitter, and the direct signal will be arriving where the minimum gain value of the antenna (-58.62 dB) occurs. On the other hand, when the transmitter is in between the AOI and the receiver, the gain is maximum because the signal is introduced to the receiver through the main beam. It is necessary to keep in mind that the transmitter uses an omnidirectional antenna.

Now, having calculated the loss of the direct signal, because of the effects of the terrain and atmosphere, and the gain introduced by the receiver antenna, it is possible to predict that the minimum signal power will occur on the regions near both AOI. The maximum value will be near the transmitter toward the negative Y-axis, or South axis.

According to equation (3.5), adding the transmitted power (52dBW app.) plus the transmitter gain (8dB), minus the propagation losses plus the receiver antenna gain, the result will represent the signal power at every coordinate of the terrain. Evaluating the aforementioned equation, yields the result presented in Figure 4.6.

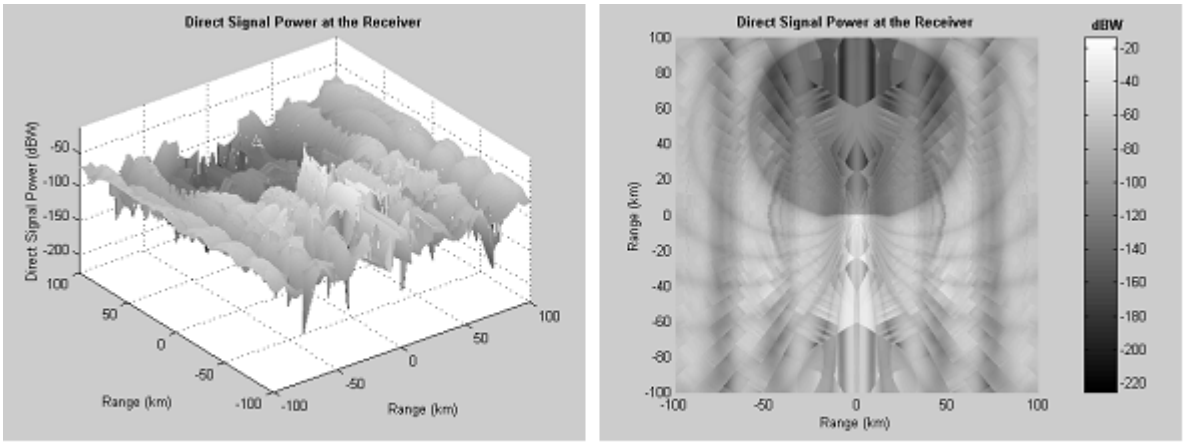

(a) (b)

Figure 4.6 Received power of the direct signal, including the effects of the receiver antenna, assuming that the receiver can be located anywhere on the terrain
(a) Elevated view. (b) Top view.

This partially solves the unknown values of the available signal within the terrain limits. The maximum value is –13.80dBW at transmitter location. The minimum value is –225.62dBW at (±20.2km, 100km).

At this stage it is possible to visualize especially in Figure 4.6(b), that the receiver looking at the AOI of the first quadrant will be located within the darkest semi-circle at the right of the X-axis 0 mark. In that region, the direct signal is not expected to be strong enough to exceed the value of the indirect signal, but is likely to have the necessary strength to activate the receiver.

4.6 The Transmitter-To-Object Path

The direct signal power was calculated above. Now the loss value of the direct signal at the specific path from the transmitter to the object is the next calculation to be performed. Therefore, it is possible to calculate the power of the signal scattered from the object.

By applying the suggested method to calculate the direct signal loss, the effects of the terrain and the atmospheric conditions generate a loss value of the signal, found to be 154.54dB. That is, when the range is 101,435km and the flight level is 4,279.8m. Then, by replacing the values of the variables on equation (3.6), the power of the scattered signal from the object is –84.55dBW. The system needs at least –180dBW (Eq. 2.15) to provide detection. This means that there is a margin of approximately 95.45dB of losses that can be accepted before the indirect signal is too weak to generate the needed information.

4.7 The Object-To-Receiver Path

The last information needed before determining the possible receiver locations, is resolving the losses of the object-to-receiver path, including the effects of the receiver antenna pattern.

As done previously on the direct path case, the propagation losses were calculated at predefined altitudes. Those levels are 5,020m, 4,770m, 4,520m, and 4,280m. The results were combined to obtain the predicted loss values 20m above the ground level.

The symmetric conditions mentioned earlier are only valid for the Y-axis. Therefore the calculations where made on the first and fourth quadrant, and the results were expanded to the whole terrain based on the assumption that the scattered signal from the object does not have enough strength to be considered beyond the main elevation along the Y-axis.

Figure 4.7 shows the losses of the scattered signal at the specific different flight levels.

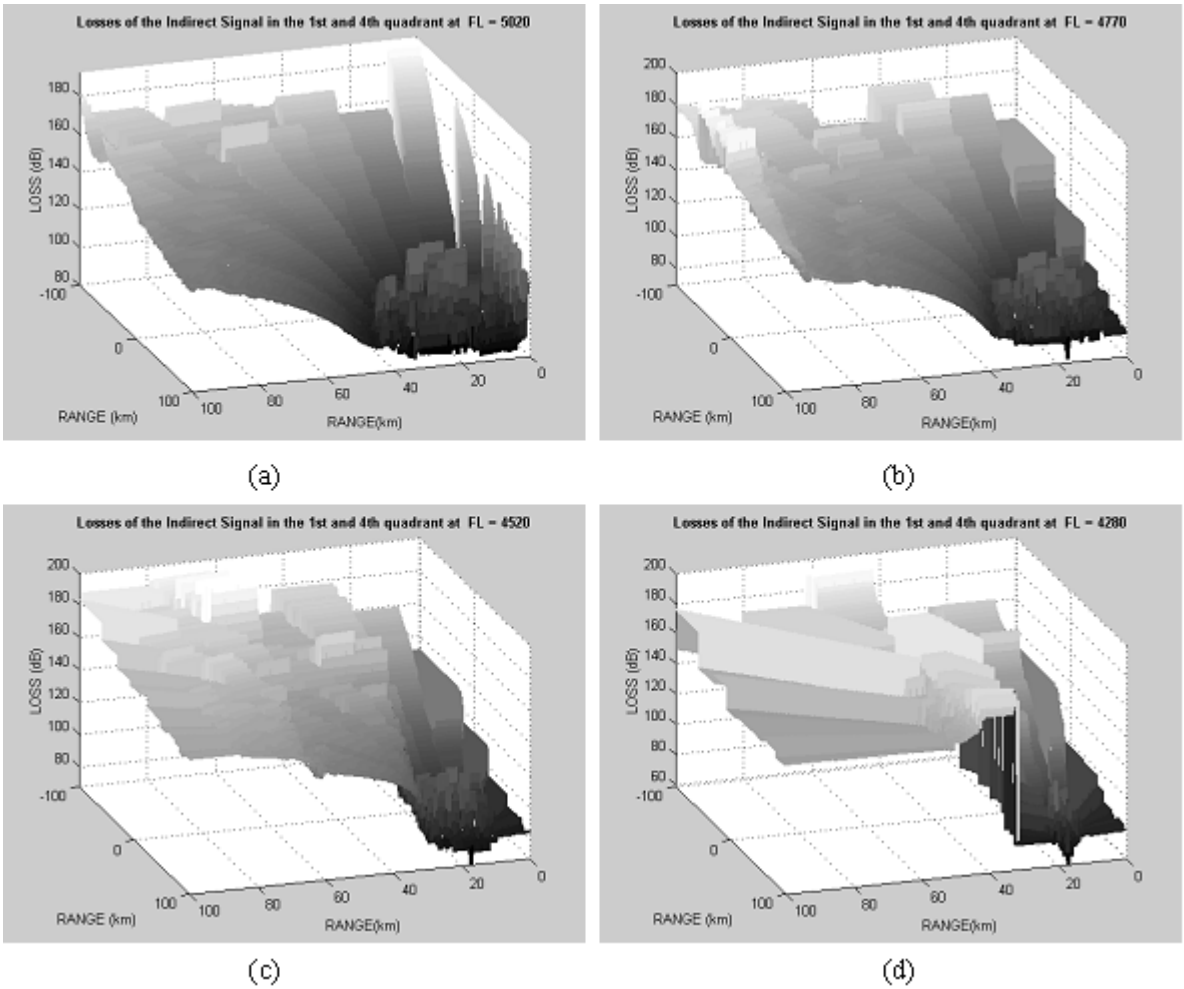

Figure 4.7 Signal propagation losses from the object, within the first and fourth quadrant at: (a) 5,050m. (b) 4,800m. (c) 4,600m. (d) 4,400m.

The plots are presented from an elevated view where the AOI is closer to the observer as seen according to the axis ranging from 100km to –100km (Y-axis). As expected, the loss is minimum at the object location and increases with distance. In addition, the value increases dramatically as the signal propagates toward the left of the object due to distance and existing elevations on the terrain. The total estimated signal loss at the receiver antenna height (20m above the ground level) is obtained from the information contained on the plots of Figure 4.7, and depicted in Figure 4.8.

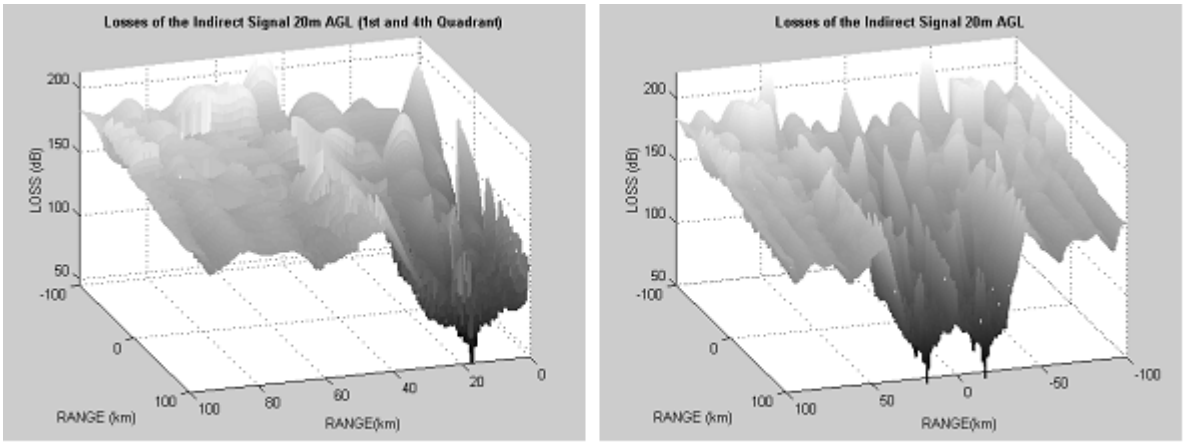

(a) (b)

Figure 4.8 Signal propagation loss, from the object at 20m above the ground level, on: (a) First and fourth quadrant. (b) Whole terrain.

The minimum value is 45.58dB at the AOI. This loss of the indirect signal is within the margin mentioned on the previous section. This implies that at least, a receiver within a few miles from the AOI, will detect a object, with a radar-cross-section of $10m^2$, flying 100m above the ground, and illuminated by the TV transmitter specified on Chapter II.

As previously done in the direct path and indicated in equation (3.7), the power of the indirect signal at the receiver is calculated by subtracting to the power of the signal *transmitted* by the object (-84.55dB), the path loss, and adding the value of the maximum gain of the receiver antenna (18.45dB). In this last term, the maximum value is considered because it is assumed that the object will be located at the antenna boresight. The resulting power values are shown next in Figure 4.9.

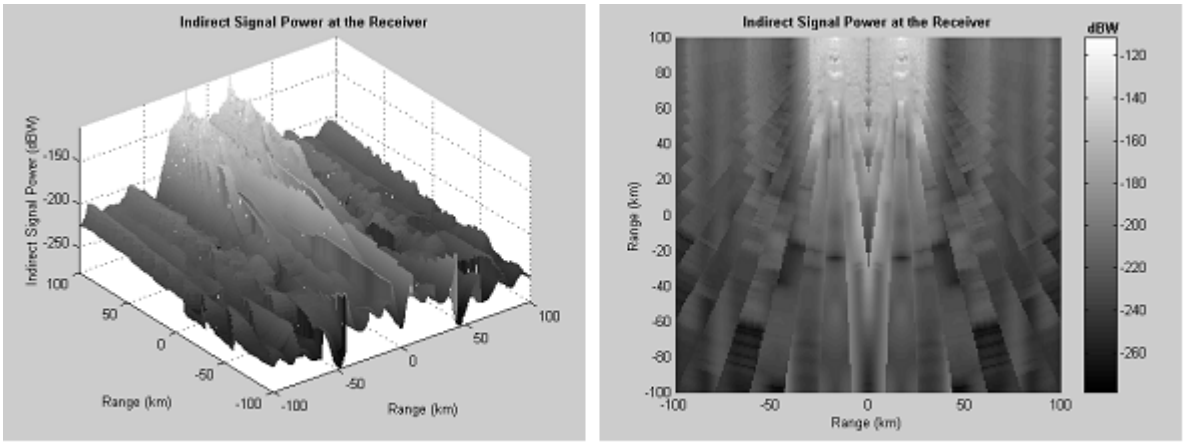

(a) (b)

Figure 4.9 Received power of the indirect signal. (a) Elevated view. (b) Top view.

These plots let see clearly that the maximum values are located near both areas of interest, and are over the threshold established by the receiver. The maximum value is –111.69dBW at each of the AOI's. The minimum value is –278.61 at the terrain coordinates (± 46.8km,-100km).

4.8 The Receiver Location.

As mentioned before, the problem of defining the receiver location on a PCL system from a technical point of view, consist basically in determining the regions where the power of the direct and indirect signal at the receiver reach an acceptable level, sufficient for processing the signal and perform detection of objects on a specific AOI.

The powers of the direct and indirect signals at every coordinate of the terrain, as well as the threshold level of the receiver are now known. The criteria for the minimum signal levels was established by equations (3.8) and (3.9). The first equation states that the indirect signal must be equal to or greater than –180dBW. The second equation states that

the direct signal, after being filtered (80dB), must be equal to or less than the indirect signal. These restrictions will determine the two sets of coordinates where the receiver can be placed. Figure 4.10 and 4.11 show the resulting areas meeting the two conditions. The final solution space will be determined by the intersection of them.

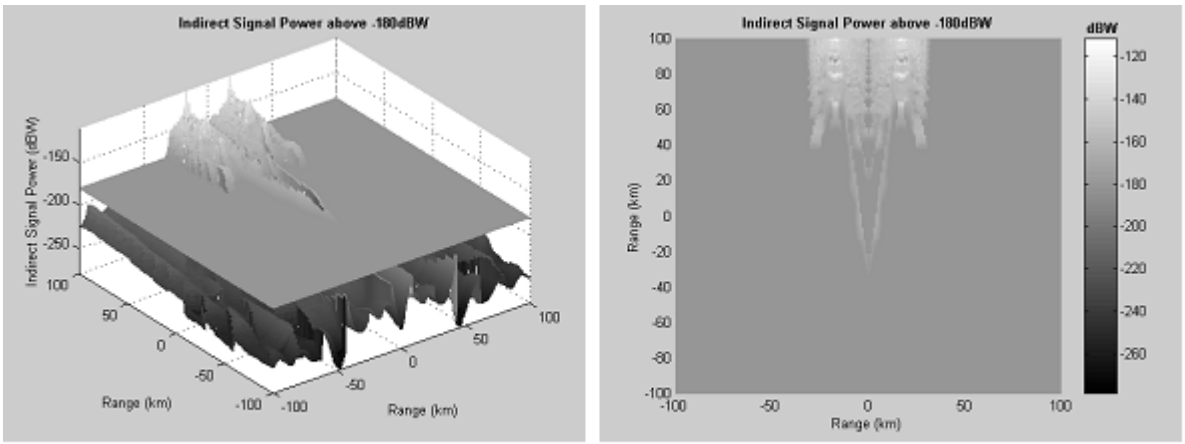

(a) (b)

Figure 4.10 Indirect signal power above the receiver threshold. The uniform gray surface specifies the threshold level. The lighter areas indicate the coordinates where the first restriction is met.

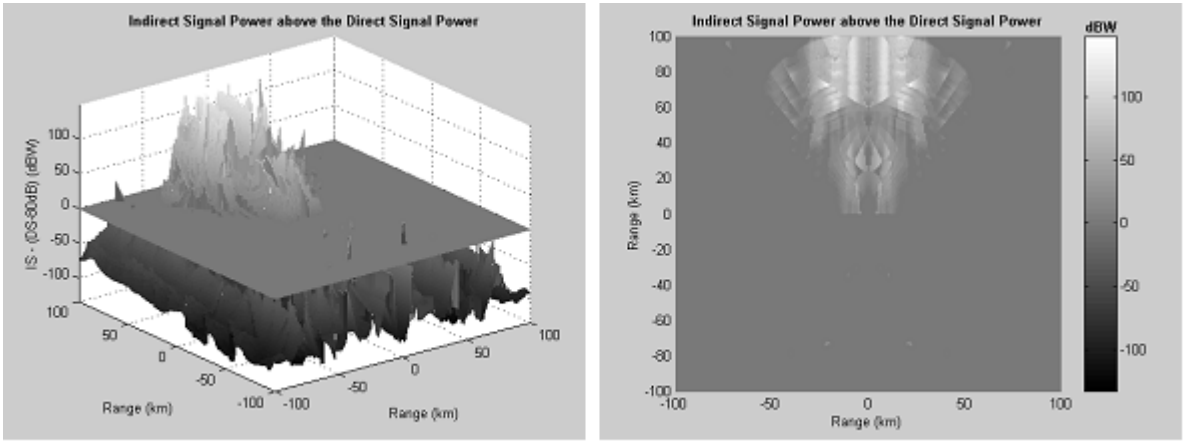

(a) (b)

Figure 4.11 Indirect signal power level above the direct signal power level. The uniform gray surface specifies the boundary level where the indirect signal is stronger than the direct signal. The lighter areas indicate the coordinates where the second restriction is met.

The intersection of the regions above the plane cutting the surfaces of Figure 4.10 and 4.11 gives the final result observed in Figure 4.12.

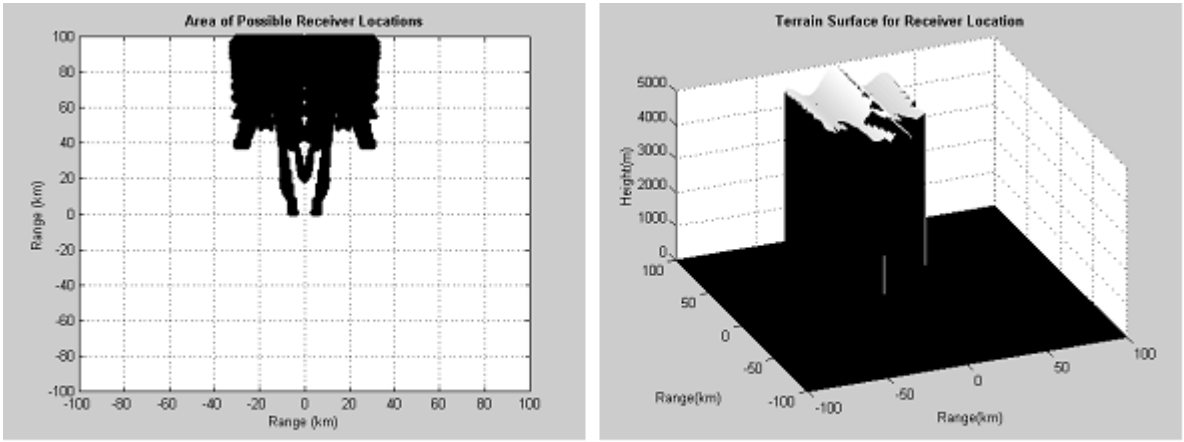

Figure 4.12 Terrain coordinates to locate the receiver of a PCL system, under the assumptions and requirements previously established.

4.9 Summary

This Chapter presented the partial results for the direct and indirect signal losses and powers, and the effect of the receiver antenna pattern on the direct signal. Finally, the criteria to determine the proper signal levels was applied and the possible receiver locations determined.

V. Conclusions and Future Work

5.1 Conclusions

This research focused on one of the many possible applications of a PCL system. Specifically, to fill the gaps of the air surveillance sensors of an air defense system. These gaps are normally generated by the topography, and are used by unauthorized objects (drug smugglers, etc) as a gate to penetrate the air space and avoid or delay detection. For the implementation of this PCL function, a method was presented to determine the possible receiver location, considering the effects on the propagation of the electromagnetic signals introduced by the terrain and the atmospheric conditions.

The output of the proposed algorithm represents the general area for locating the receiver site. The resulting data is the space solution of the coordinates where a particular receiver can detect a object flying over the terrain, at a specific point previously defined.

The incorporation of software such as AREPS, which accounts for the aforementioned effects, gives a realistic approach to the problem of implementing a PCL system while providing a more accurate solution.

The proposed algorithm represents a flexible solution to the problem. In addition to the use of a customized terrain, AREPS allows the use of digital terrain elevation data (DTED) files which actually simplifies the calculations. Use of DTED files saves the work and time required to generate each of the terrain files. AREPS automatically calculates the propagation loss at a set of predefined bearings. In addition, this software permits the introduction of local atmospheric conditions into signal loss predictions. Therefore, the site

analysis for the receiver fits that specific region, without the need to use any general atmospheric model.

Another benefit of the algorithm, in terms of its flexibility, is that it allows calculations for analog TV signals, as well as, as digital television and radio broadcast signals.

The fact that all possible receiver locations are resolved allows for analysis from different operational and technical points of view. An optimal receiver location was not determined due to the broadness of possibilities involving the word *optimal*. As presented in the first part of this thesis, the realm of operational applications and technical constraints on a PCL system are wide. Thus, an optimal solution varies for each specific operational requirement. An optimized specific location could be determined from data generated by this algorithm, but previous definitions of the general objectives (operational and technical) will be needed.

For example, in the operational field, to increase the probability of detection of an object with high ambient clutter, a large bistatic angle β is desired (β~180º). This requirement increases the bistatic radar-cross-section σ_B as explained in Chapter II. To somehow manipulate the value of this angle, the following aspects need to be taken into account. Equation (2.7) establishes that the bistatic angle is given by the difference between the angles θ_T and θ_R, representing the angle from the North-axis to the object with respect to the transmitter, and the angle from the North-axis to the object with respect to the receiver, respectively. In the scenario stated in this thesis, where the AOI is a fixed point, θ_T is also fixed. Then it is necessary to increase θ_R. This requisite is met by locating the receiver as far as possible from the transmitter and from the object path. If the idea is to maximize the bistatic angle value (180º) the object should cross the base line. Then the

receiver should be placed anywhere East of the penetration path of the object (X = 17km). Given that the goal is to provide early detection, for this type of plane, the receiver needs to be as far North as possible so that the base line crossing occurs earlier. Then the receiver should be as close as possible from the line joining the transmitter and the AOI. Figure 5.1 shows the values of the bistatic angle at each coordinate where the receiver could be located.

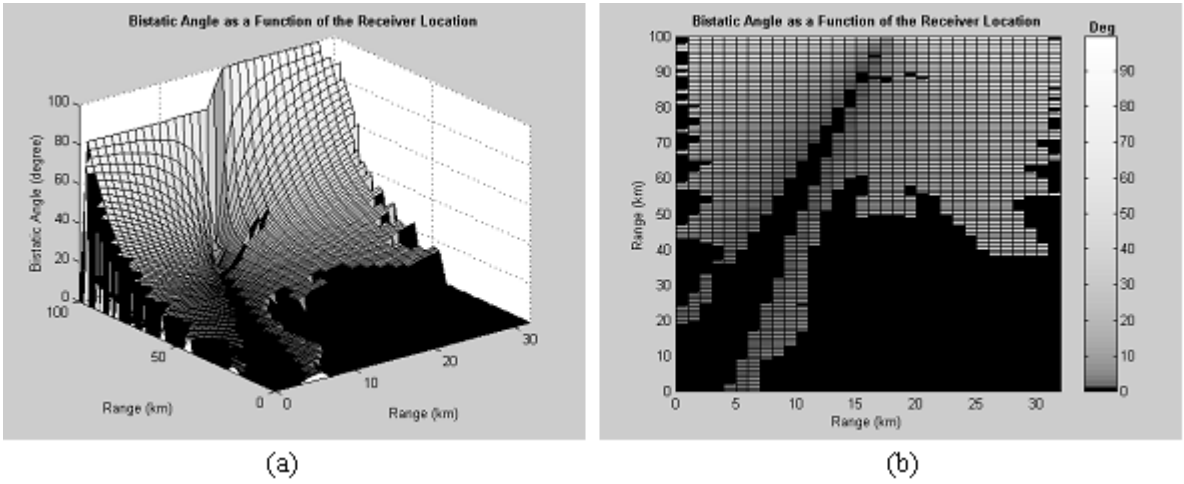

Figure 5.1 Bistatic angle as a function of the receiver location. (a) The lighter zones represent the location for operations where an increased object radar-cross-section is needed. (b) Top view.

On the other hand, for the quasi-monostatic and bistatic regions, the bistatic radar-cross-section of a object is always smaller than the corresponding monostatic value, and it decreases with the increment of β. The best case occurs within the quasi-monostatic region ($0^\circ < \beta < 5^\circ$). Figure 5.2 shows the coordinates where this situation occurs.

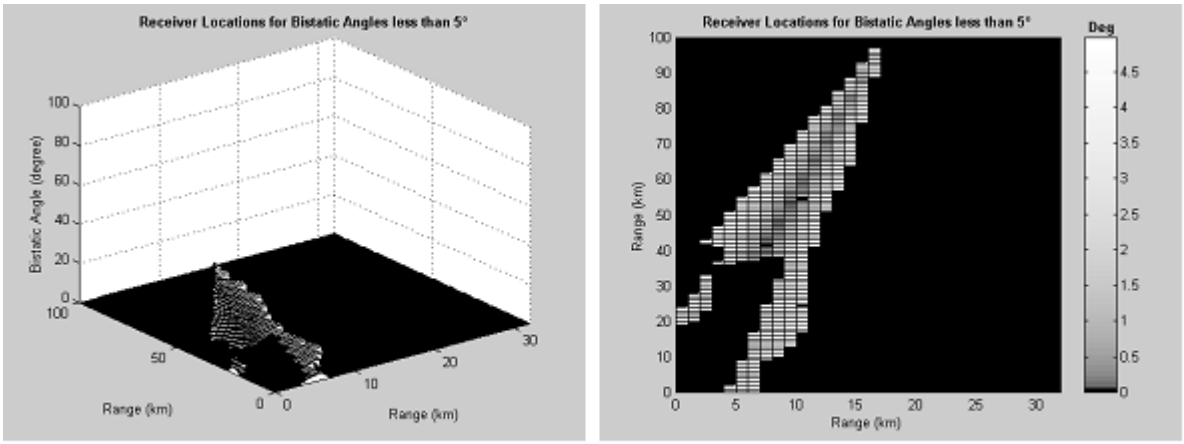

(c) (d)

Figure 5.2 Quasi-monostatic region. (a) The closest coordinates to the imaginary line joining the transmitter location (0,0) and the AOI (17,100) form the smallest bistatic angle. As the separation increase, so does the angle. (b) Top view.

The previous suggested general receiver locations, only treat the radar-cross-section problem and disregard any other operational or technical constraints like, for example, the amount of time the object could be within the receiver coverage region.

In the technical field, the need for better Doppler information could arise. Here, different criteria are used. According to equation (2.8), the value of the Doppler shift is a function of the bistatic bisector, and of the angle formed by the velocity vector and the bistatic bisector. The smaller the angles the larger the Doppler shift. The larger the Doppler shift, the larger the separation of the peaks on the frequency spectrum of the direct and indirect signal. Then maximum value will occur in any of the locations that maximizes the product $\cos(\delta)\cdot\cos(\beta/2)$. The minimum value of the Doppler shift will be when the object cross or fly along the base line. Figure 5.3 shows the value of the angle δ as a function of

the receiver location, and the value of the Doppler shift generated on the signal by the object at the AOI and flying at 400knots on a straight line southward.

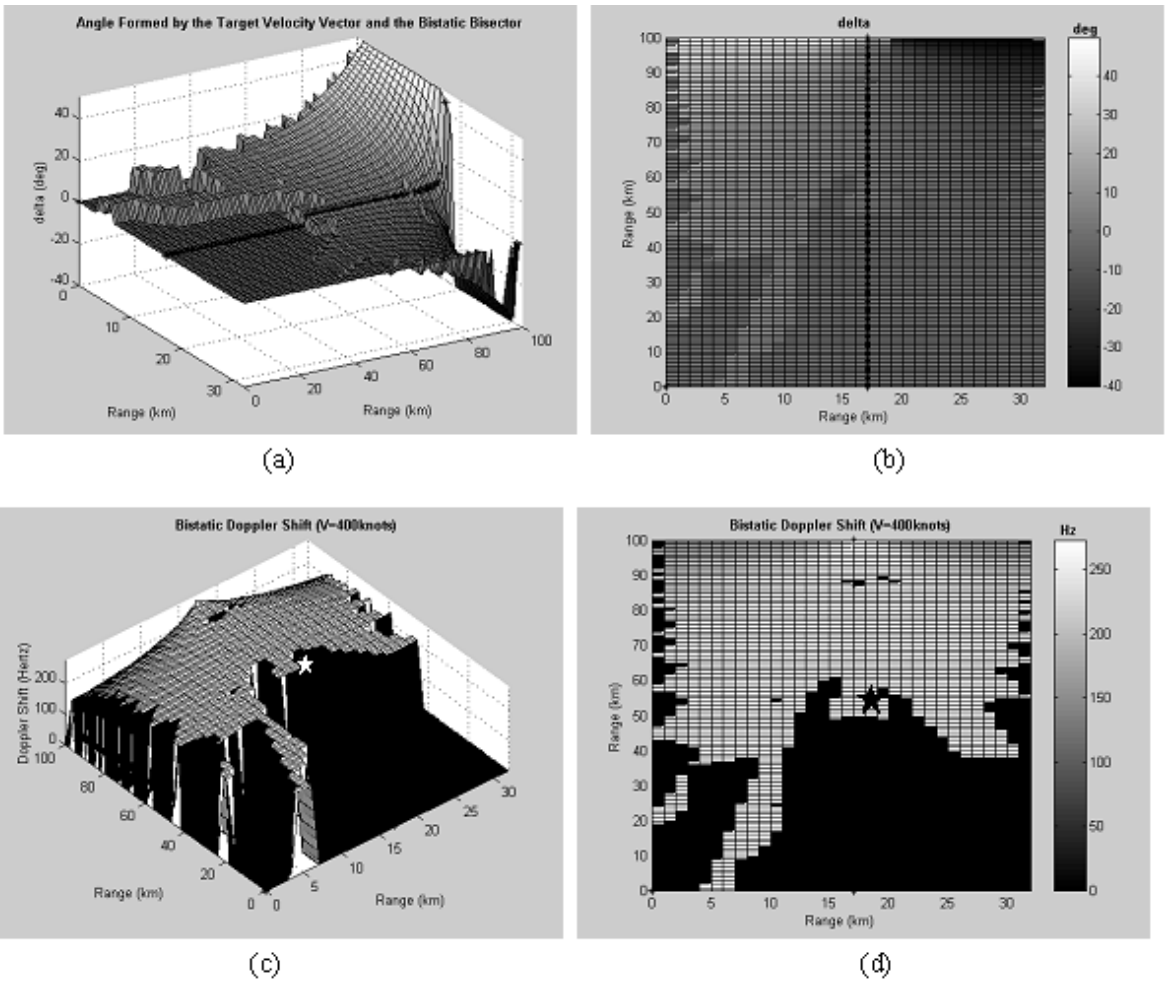

Figure 5.3 The angle formed by the object velocity vector and the bistatic bisector, and the resulting Doppler shift. (a) Surface showing the δ values on the possible receiver locations. The smallest absolute values of the angle δ occur near the object path at its right. (b) Top view. The black line marks the object path. (c) Surface showing the Doppler shift values. The white star shows the receiver location to obtain the maximum value. (d) Top view.

Another technical consideration that will determine the location of the receiver in this type of scenario is the object path dynamic range. This concept can be understood as the

difference between maximum and minimum signal-to-noise ratio along the object path, assuming a constant bistatic radar-cross-section and thermal noise [2:75]. Then, the receiver location will drive the maximum and minimum values of signal-to-noise ratio. Therefore, according to the hardware capabilities used, the limit values of signal-to-noise ratio will limit the possible locations.

Other technical and operational matters could be considered when deciding the receiver location by following the same scenario used throughout this thesis. However, by using the methodology introduced in this research, the necessary data to define the geographical regions where certain parameters meet a particular number of restrictions is now available.

5.2 Future Work

This research effort proposed a method to obtain the necessary information to perform a more detailed analysis on the receiver location of a PCL system based on technical and operational constraints and requirements. Future work should concentrate on processing the obtained data, and on the analysis of the effects of changing the scenario in terms of adding more receivers and/or transmitters.

In particular, there are a number of research areas that can be derived from this study. Among them, the following are some examples.

First, there are several ways to analyze and independently determine a suitable location for a receiver on a PCL system. In reality, several conditions must be met simultaneously for a successful particular application. Then a study to optimize the receiver location must be performed. This optimization can be seen as a multiobjective problem, where for

example, a specific range of bistatic angle is needed, a particular baseline length must not be exceeded, and certain minimum Doppler shift value can be processed, etc. The optimal solution could be found using genetic algorithms. This method will require the definition of objectives as the ones just described, the decision space, and the constraints. The result will describe the best receiver locations where the objectives are met. Within this area, including the dynamics of a moving object will induce changes on the bistatic radar-cross-section. An adequate object model and the use of genetic algorithms will make possible the optimization of the receiver location in terms of obtaining the strongest object echoes.

Second, the extension from a bistatic case, similar to the one presented here, to a multistatic situation with more than one receiver and/or more than one transmitter can be a second matter of research. This situation will vary the size of the solution space. Even though the number of possible scenarios will also increase, the fact that there will be more electromagnetic sources in the environment could limit the solution space due to the interference caused by the direct signal.

A third area to take the results a step closer to reality, is to perform an analysis of the interpolation/extrapolation methods used to obtain the losses at a specific value above the ground. When calculating the loss matrix at a specific flight level from individual loss vectors at a certain bearing the Matlab® command *griddata* was used. This instruction interpolates the surface formed by the loss vectors at the points specified by the original terrain grid defined by the matrices **X** and **Y**. The resulting loss matrix represented a surface, as those shown in Figures 4.3 and 4.7. The interpolation method used was *nearest.* The interpolation/extrapolation command and method used to calculate the signal loss 20m above the ground was *interp1* and *spline* respectively. Both methods were selected because

they offered a real value at every coordinate. In many cases, the other methods would give a value of *NaN* (Not a Number), or values that did not reflect reality. Improving these procedures by making a piecewise interpolation or developing an independent interpolation algorithm could refine the results and have an impact on the accuracy of the loss levels, and therefore on the available signal powers.

Finally, the implementation of a real PCL system, where the receiver site would be located on the coordinates determined by the application of the method developed in this thesis, could provide the necessary data to validate the results. The difference of the signal powers, encountered in a real model could serve to establish a correction factor.

Appendix A: Matlab® Codes

The following is a list of the Matlab® codes used throughout this thesis to obtain the results and generate the plots. The numbers at the end of the file names indicate the sequence in which they are used, according to the methodology proposed in Chapter 3. The letters HR and LR indicate when the code generates a High Resolution result (terrain defined every 100m) and a Low Resolution result (terrain defined every 1000m), respectively.

- terrain_generation_1.m
- smooth_terrain_2.m
- Filter_DSL_AREPS_output_3.m
- matrix_LD_at_all_h_4.m
- matrix_LD_at_all_h_HR_4.m
- Direct_Signal_Loss_5.m
- Direct_Signal_Loss_HR_5.m
- antenna_pattern.m
- AOA_of_DS_at_ANT_1_4Quad_7.m
- AOA_of_DS_at_ANT_1_4Quad_HR_7.m
- Antenna_Gain_8.m
- Antenna_Gain_HR_8.m
- Direct_Signal_Power_LRandHR_9.m
- power_at_target_10.m
- terrain_generation_centered_at_AOI_11.m

– smooth_terrain_AOI_12.m

– Filter_ISL_Areps_output_13.m

– matrix_LI_at_all_h_14.m

– matrix_LI_at_all_h_HR_14.m

– Indirect_Signal_Loss_15.m

– Indirect_Signal_Loss_HR_15.m

– Indirect_Signal_Power_16.m

– Indirect_Signal_Power_HR_16.m

– Total_Signal_Power_17.m

– Total_Signal_Power_HR_17.m

– BmatrixAOI_18.m

– BmatrixAOI_HR_18.m

– B_from_0_to_5_19.m

– delta_20.m

– doppler_21.m

The files are stored on a CD. There are two copies; one with the author (see *permanent address* on VITA) and one with the Thesis Advisor (Professor Andrew J. Terzuoli, Jr. Office: (937) 255-3636 x 4717 Air Force Inst of Tech).

Bibliography

References

1. Howland, Paul E., "Television Based Bistatic Radar", PhD. Thesis, University of Birmingham, England, September 1997.

2. Willis, Nicholas J. *Bistatic Radar* (2nd Edition). Silver Spring, MD. Technology Service Corporation, 1995.

3. Advanced Propagation Model. Version 1.30.0.1. Computer software. Space and Naval Warfare Systems Center, Atmospheric Propagation Branch, San Diego CA, July 25, 2001.

4. Advanced Refractive Effects Prediction System. Version 2.1.2007, IBM compatible, 12.55 Mbytes. Amelia Barrios and others. Computer software. Space and Naval Warfare Systems Center, Atmospheric Propagation Branch, San Diego CA, July 25, 2001.

5. Patterson, Wayne L. Advance refractive Effects Prediction System (AREPS). Version 2.0 User's Manual. Technical Document 3101. Space and Naval Warfare Systems Center, S, Atmospheric Propagation Branch, San Diego CA, January 2000.

6. Sailors, D.R., Amelia Barrios, and others. Advanced Propagation Model (APM) Computer Software Configuration Item (CSCI) Documents. Technical Document 3003. Space and Naval Warfare Systems Center, Atmospheric Propagation Branch, San Diego CA, August 1998.

7. Barrios, Amelia E. "A terrain parabolic equation model for propagation in the troposphere" *IEEE Trans. Antennas and Propagation*, Vol. 42, No. 1, pp. 90-98, January 1992.

8. Kuttler, J.R. and G.D. Dockery, "Theoretical description of the parabolic approximation/Fourier split step method of representing electromagnetic propagation in the troposphere." *Radio Sci*., pp. 381-393, Mar-Apr. 1991.

9. Dockery, G. Daniel "Modeling electromagnetic wave propagation in the troposphere using the parabolic equation." *IEEE Trans Antennas and Propagation*, Vol. 36, No. 10, pp. 1464-1470, October 1988.

10. Benson, K. Blair. *Television Engineering Handbook*. New York, NY. Mc Graw Hill, 1986.

11. Skolnik, Merrill I. *Radar Handbook* (2^{nd} Edition). New York, NY. Mc Graw Hill, 1990.

12. Lesturgie, M. and D. Poullin "Frequency Allocation in Radar: Solutions for Low Frequency Band", Colloque International sur les Systemes Radar – RADAR'99 Brest, France, May 18-20, 1999

13. Poullin, Dominique. "On the Use of COFDM Modulation (DAB, DVB) for Passive Radar Application". Office National d'Etudes et Recherches Aeroespatiales (ONERA). Internal report.

14. Stutzman, W. and G. Thiele. *Antenna Theory and Design* (2nd Edition). New York, NY. John Wiley & Sons Inc., 1998.

15. Balanis, C. *Antenna Theory, Analysis and Design* (2nd Edition). New York, NY. John Wiley & Sons Inc., 1998.

Vita

Lt Carlos A. Meier was born in Temuco, Chile in 1972. He graduated from "Bautista" High School in 1989 and from the Chilean Air Force Academy in 1994. He earned a degree as an Electrical Engineer in March 2000.

His first assignment was the Communications and Detection Group Nº32 (1997-1999) where he performed different functions as a communication officer and a crew member of AEW systems, designing and deploying the communication system for operations to Antarctica, Ester Island and the Chilean mainland. In 1999 he graduated from the course "Electronic Warfare" for officers. In 2001 he was assigned to the Education Division to enter the Graduate Electrical Engineer Program at the U.S. Air Force Institute of Technology. Upon AFIT graduation, he will be assigned to the Aeronautic Polytechnic Academy.

Permanent Contact Address:

Fuerza Aérea de Chile
División de Educación
Gran Avenida J. M. Carrera, Paradero 32 1/2
El Bosque, Santiago
Chile
Phone: 56-2-5402604

REPORT DOCUMENTATION PAGE

Form Approved
OMB No. 074-0188

1. REPORT DATE *(DD-MM-YYYY)*	**2. REPORT TYPE**	**3. DATES COVERED** *(From – To)*
26-03-2002	Master's Thesis	1 Sept 2001 – 28 Feb 2002

4. TITLE AND SUBTITLE

DETERMINATION OF THE POSSIBLE LOCATIONS OF THE RECEIVER ON A PASSIVE COHERENT LOCATION SYSTEM, CONSIDERING THE EFFECTS OF THE TERRAIN AND THE ATMOSPHERIC CONDITIONS.

5a. CONTRACT NUMBER

5b. GRANT NUMBER

5c. PROGRAM ELEMENT NUMBER

6. AUTHOR(S)
Meier, Carlos A. Lt, Chile Air Force

5d. PROJECT NUMBER

5e. TASK NUMBER

5f. WORK UNIT NUMBER

7. PERFORMING ORGANIZATION NAMES(S) AND ADDRESS(S)
Air Force Institute of Technology
Graduate School of Engineering and Management (AFIT/EN)
2950 P Street, Building 640
WPAFB OH 45433-8865

8. PERFORMING ORGANIZATION REPORT NUMBER
AFIT/GE/ENG/02M-17

9. SPONSORING/MONITORING AGENCY NAME(S) AND ADDRESS(ES)
Paul E. Howlland
NATO C3 Agency
Surveillance Branch
AirC2 Sensors División
P.O. BOX 174, 2501 CD
The Hague, Netherlands. Tel: 31- (0) 70-374-3752
e-mail: Paul.Howland@nc3a.nato.int

10. SPONSOR/MONITOR'S ACRONYM(S)

11. SPONSOR/MONITOR'S REPORT NUMBER(S)

12. DISTRIBUTION/AVAILABILITY STATEMENT
APPROVED FOR PUBLIC RELEASE; DISTRIBUTION UNLIMITED.

13. SUPPLEMENTARY NOTES

14. ABSTRACT It has always been an issue for an armed force, or government, to obtain complete radar coverage over an area of interest. Generally, this objective remains unaccomplished due to geographical, technical, and/or operational reasons (meaning topographic obstacles, transmitted power, extreme isolation, hierarchy of objectives, etc.) The fact of having vast areas of territory beyond radar coverage can be decisive in an armed conflict.

With the recent resurgence of bistatic radar theory and applications, now in the form of Passive Coherent Location (PCL) systems, using existing signal sources (TV and Radio stations) it is possible to decrease the blind zones of a country's air defense system, in a somehow economic and effective way.
The general purpose of this thesis is to develop a methodology to determine possible receiver locations needed to implement a PCL system, while emphasizing low altitude coverage, specific terrain and atmospheric information, available signal sources and the need for coverage.

15. SUBJECT TERMS
Radar – Passive Sensors – Radar Site Analysis – Atmospheric Propagation Loss.

16. SECURITY CLASSIFICATION OF:			**17. LIMITATION OF ABSTRACT**	**18. NUMBER OF PAGES**	**19a. NAME OF RESPONSIBLE PERSON**
a. REPORT	**b. ABSTRACT**	**c. THIS PAGE**			Andrew J. Terzuoli (ENG)
U	**U**	**U**	**UU**	117	**19b. TELEPHONE NUMBER** *(Include area code)* (937) 255-3636 X 4717